TU Delft
Delft University of Technology

Hybrid solution for the response of a rod with varying foundation stiffness subjected to a uniformly moving constant load

M.Sc. - Additional thesis project

Delft, 2017

Student:

Andrei B. Faragau (4519116) — Steel and Timber Structures

Committee members:

Prof. Dr. AV Metrikine (chairman) — Head of Offshore Engineering

Chair Dynamics of Solids and Structures

Dr. ir. K.N. van Dalen — Structural Mechanics

Ir. J.S. Hoving — Offshore Engineering


TU Delft
Delft University of Technology

TU Delft
Delft University of Technology

Table of contents


TU Delft
Delft University of Technology

1. Abstract

Trains passing from a low stiffness medium, such as the soil, to a relatively high stiffness bridge will induce dynamic behaviour in the structure. This phenomenon is referred to as 'transition radiation' and has been demonstrated theoretically as early as 1945 by Vitaly Ginsburg and Ilya Frank, in electromagnetics. As the name implies, due to the change in stiffness, there are waves propagating away from the transition. This phenomenon becomes increasingly important for train infrastructure as the trains become faster.

The velocity of the trains, nowadays, approach the velocity of elastic waves in some types of soils leading to an important amplification in displacements and stresses within the infrastructure. For this reason, the phenomena must be studied in more detail, in order for the future designs of the infrastructure to better account for this type of behaviour.

This additional thesis will tackle a small part of this complex phenomena, namely making an one dimensional model of a rod resting on elastic foundation, which exhibits smooth varying stiffness, subjected to a uniformly moving constant load. Although the system represents a rod, it can easily be extended to represent a beam. Semi-analytical methods are used to solve the system. More precisely, using Laplace transform, the governing equation is expressed in Laplace domain, where the second spatial derivative is approximated using Finite Difference Method, due to the smooth varying stiffness.

If this model were to be feasible to extend to two or three dimensions, the computational power required to solve the system must be minimum, thus the computational domain has to be reduced as much as possible. While doing so, several challenges have been presented, as it will be seen in the paper. These challenges have been divided in two main chapters:

3) Finding the non-reflective boundaries
- As soon as the system is solved using numerical methods, the computational domain has to be finite. But because the railway track can be considered practically infinite, the finite domain has to exhibit the same behaviour as the infinite system. Consequently, some type of non-reflective boundaries have to be found and implemented.

4) Finding the initial state of the rod at the moment of the load entering the computational domain
- Due to the smooth varying stiffness, the initial state, the state of the system exactly when the load enters the computational domain, is different than the one found in the steady-state solution. For this reason, deriving it required a different approach base on the Reciprocity theorem.

2. Problem statement

As has been discussed in the abstract, the scope of this additional thesis is to develop a numerical model of an infinite rod resting on an elastic foundation with space dependent stiffness, subjected to a constant moving load with constant velocity, as seen in the following drawing.

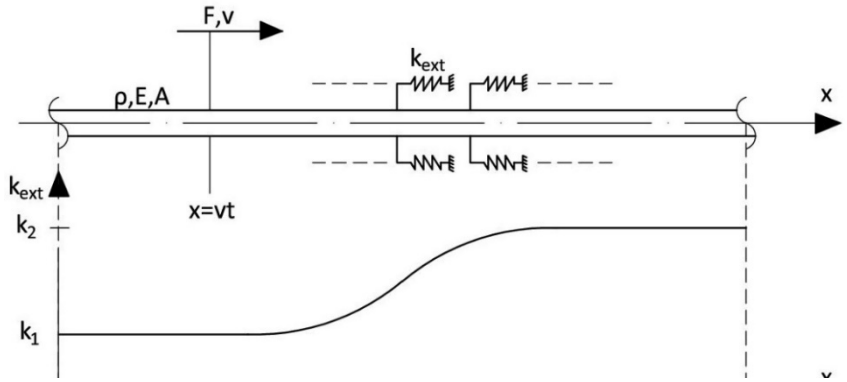

Figure 1 - Infinite rod resting on elastic foundation with varying stiffness subjected to a uniformly constant moving load

One should realise that an infinite system cannot be modeled numerically. To go around this issue the length of the rod has to be truncated to a finite value, but at the same time the resulting system should exhibit the same behaviour as the infinite system. This can be done by bounding the rod with some non-reflective boundaries, as seen in the following figure.

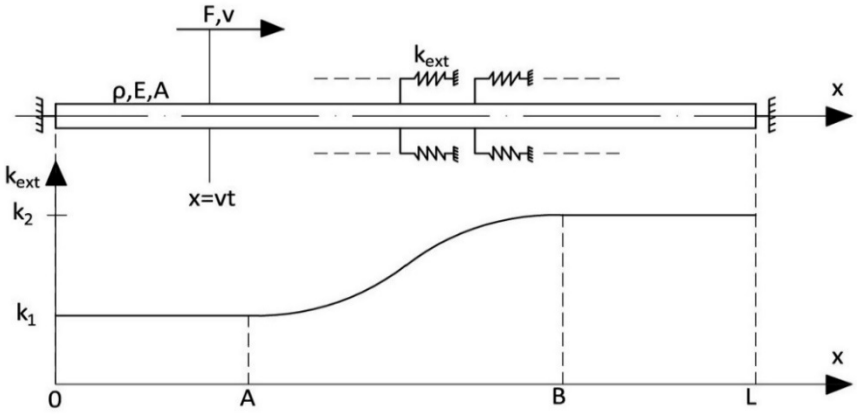

Figure 2 - Finite rod resting on elastic foundation with varying stiffness subjected to a uniformly constant moving load

Now the question arises of how long should the computational domain be? As the domain becomes smaller, the computational power needed decreases, thus the domain should be as small as possible. In this additional thesis, we propose to reduce the computational domain from the point where the stiffness starts to vary (point A fig.2) to the point where it stops (point B fig.2).

Due to the smooth transition of stiffness in space the system is solved using the Finite Difference Method to approximate the second order derivative with respect to space. As a first step, the system with constant stiffness is going to be analysed, the subject of the next chapter.

3. Deriving the non-reflective boundaries of the system with constant external stiffness

In the first case the steady-state solution of the system will be derived to get some insight into the behaviour of the system under a moving load. Afterwards, the steady-state and transient solutions are going to be derived for the finite system by introducing the non-reflective boundaries.

3.1. Steady-state solution for the infinite rod on elastic foundation with constant stiffness

The system can be solved by introducing a moving reference frame with the origin at the position of the load and splitting it up in two domains: domain 1 for $x < vt$ and domain 2 for $x > vt$, where v represents the velocity of the load.

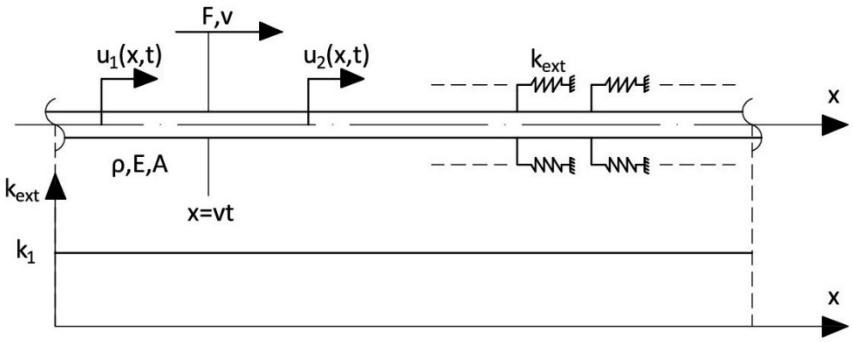

Figure 3 – Infinite rod on elastic foundation with constant stiffness subjected to a uniformly moving constant load

The governing equation has to be formulated. Generally, this is comprised by the equations of motion, boundary conditions, interface conditions and initial conditions. In this case, because the steady-state solution is sought for, the effects of the initial conditions on the solution have already passed.

The equations of motion for the two domains read:

$$\frac{\partial^2 u_1(x,t)}{\partial t^2} - c^2 \frac{\partial^2 u_1(x,t)}{\partial x^2} + \omega_0^2 u_1(x,t) = 0 \qquad \text{for } x < vt$$

$$\frac{\partial^2 u_2(x,t)}{\partial t^2} - c^2 \frac{\partial^2 u_2(x,t)}{\partial x^2} + \omega_0^2 u_2(x,t) = 0 \qquad \text{for } x > vt$$

- $\omega_0 = \sqrt{\frac{k_d}{\rho A}}$ represents the cut-off frequency of the system
- $c = \sqrt{\frac{E}{\rho}}$ represents the wave velocity in the rod
- k_d represents the stiffness of the distributed springs
- ρ, E, A represent the density, elastic modulus and cross-sectional area of the rod

For an easier read the time derivative is going to be replace by a dot and the space derivative by a dash. Also, the variables of the functions, x and t are going to be omitted from the writing in expressions. The equations of motion become:

$$\ddot{u}_1 - c^2 u_1'' + \omega_0^2 u_1 = 0 \qquad \text{for } x < vt \tag{1}$$

$$\ddot{u}_2 - c^2 u_2'' + \omega_0^2 u_2 = 0 \qquad \text{for } x > vt \tag{2}$$

The interface conditions read:

$$u_1 = u_2 \qquad \text{at } x = vt \tag{3}$$

$$\left(c^2 - v^2\right)\left(u_1' - u_2'\right) = \frac{F_0}{\rho A} \qquad \text{at } x = vt \tag{4}$$

- F_0 represents the amplitude of the moving load

The interface conditions represent the continuity in displacements between the two domains and the equilibrium of forces, respectively.

The boundary conditions at $x \to \pm\infty$ read:

$$u_1 < \infty \qquad \text{for } x \to -\infty, t \neq -\infty \text{ and } \left(x - vt\right) \to -\infty, t = -\infty \tag{5}$$

$$u_2 < \infty \qquad \text{for } x \to +\infty, t \neq +\infty \text{ and } \left(x - vt\right) \to +\infty, t = +\infty \tag{6}$$

These conditions represent specific restrictions for the behaviour of the motion at infinite distance. If the motion has an exponentially decaying/increasing character, then the boundary conditions state that the displacements have to decay exponentially away from the load and not increase exponentially. In other words, that the displacement at infinite distance away from the load have to be finite. Otherwise, if the motions induced by the load are waves propagating through the rod, the boundary conditions state that waves cannot travel back from $\pm\infty$ towards the load. This condition is called the radiation condition.

With the equations of motion (1) and (2), the interface conditions (3) and (4) and the boundary conditions (5) and (6) the governing equation has been formulated and mathematically the problem is determined properly.

The steady-state solutions to the equations of motion, eq. (1) and (2), have a harmonic wave form.

$$u_1 = A_1 e^{i(\omega t - kx)} \tag{7}$$

$$u_2 = A_2 e^{i(\omega t - kx)} \tag{8}$$

- A_1, A_2 represent the amplitudes of the harmonic waves
- ω represents the frequency of the harmonic waves
- k represents the wavenumber of the harmonic waves

By replacing expressions (7) and (8) in the equations of motion, one will obtain the dispersion equation eq. (9), which is the same for both domains.

$$c^2 \cdot k^2 - \omega^2 + \omega_0^2 = 0 \tag{9}$$

The phase of the wave is defined as $\phi = \omega t - kx$. For the wave to be harmonic the phase has to be constant. Consequently, its derivative with respect to time has to be zero.

$$\frac{d\phi}{dt} = \omega - k\frac{dx}{dt} = 0 \tag{10}$$

Meanwhile, the load is traveling with the velocity v and it is located for each time moment at $x = v \cdot t$. The derivative with respect to time of this expression is $\frac{dx}{dt} = v$, the velocity of the load. Replacing this result in previous expression (13), one will obtain:

$$\omega = k \cdot v \tag{11}$$

This expression is called kinematic invariant. With a system of two algebraic equations represented by the kinematic invariant (11) and the dispersion equation (9) the expressions for the frequency and wavenumber are obtained, eq. (12) and (13), respectively.

$$\omega_{1,2} = \mp \frac{v \cdot \omega_0}{\sqrt{v^2 - c^2}} \tag{12}$$

$$k_{1,2} = \mp \frac{\omega_0}{\sqrt{v^2 - c^2}} \tag{13}$$

Depending on the velocity of the load in comparison with the velocity of the waves in the rod, two cases can be distinguished: the subsonic case ($v < c$) and the supersonic case ($v > c$). In this additional thesis paper the only case considered is the subsonic case. Thus, the expressions for the frequency and wavenumber become:

$$\omega_{1,2} = \pm i\beta v \tag{14}$$

$$k_{1,2} = \pm i\beta \tag{15}$$

- $\beta = \frac{\omega_0}{\sqrt{c^2 - v^2}}$ represents the wavenumber of the eigenfield

Employing the expressions for the frequency and wavenumber in the displacement expressions (9) and (10) they become:

$$u_1 = A_1 \cdot e^{-\beta(x-vt)} + B_1 \cdot e^{\beta(x-vt)} \tag{16}$$

$$u_2 = A_2 \cdot e^{-\beta(x-vt)} + B_2 \cdot e^{\beta(x-vt)} \tag{17}$$

It can be observed from the expressions (16) and (17) that for the subsonic case the motion doesn't have a propagating character. Accounting for the proper behaviour at $x \to \pm\infty$, by employing the boundary conditions, eq. (16) and (17) reduce to:

$$u_1 = B_1 \cdot e^{\beta(x-vt)} \tag{18}$$

$$u_2 = A_2 \cdot e^{-\beta(x-vt)} \tag{19}$$

At this point the only unknowns are the amplitudes. These can be found by substituting the expressions of the displacements (18) and (19) into the interface conditions, eq. (3) and (4), thus obtaining a system of two algebraic equations.

$$\beta\left(c^2 - v^2\right)\left(B_1 + A_2\right) = \frac{F_0}{\rho A} \tag{20}$$

$$B_1 = A_2 \tag{21}$$

Solving this system of equations for the amplitudes B_1, A_2 and combining the two domains by using the absolute value $|x - vt|$, the expression for the eigenfield is obtained.

$$u(x,t) = \frac{1}{2}\frac{F_0}{\rho A}\frac{\beta}{\omega_0^2}e^{-\beta|x-vt|} \tag{22}$$

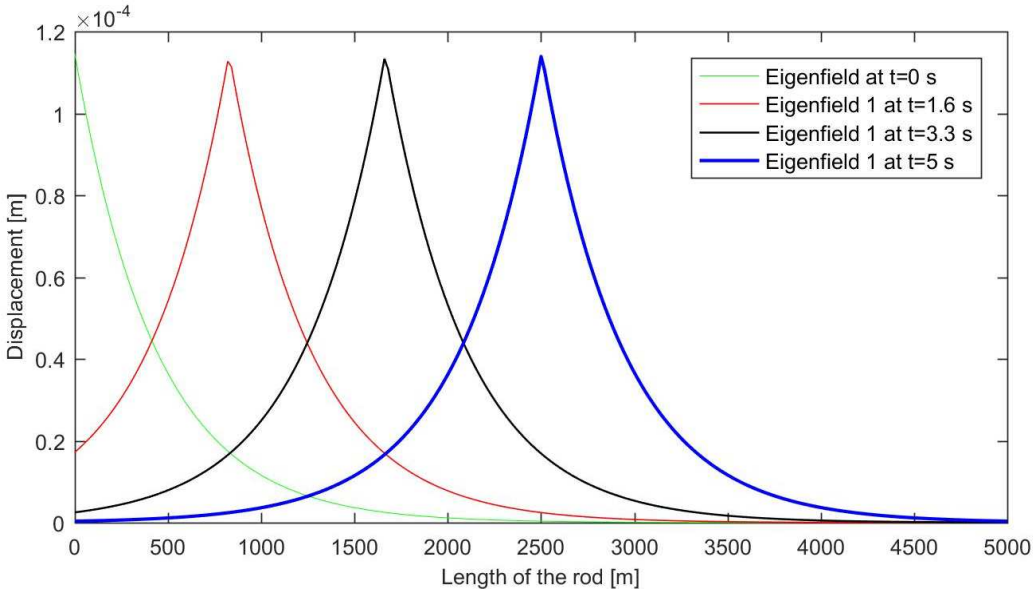

Figure 4 - Steady-state eigenfield at different time moments

It can be observed from Figure 4 that the displacement field, in the subsonic case, is symmetric with respect to the load and the field travels along with the load, being stationary with respect to it. Thus, it doesn't exhibit any radiation or propagating behaviour.

In the next subchapter, the steady-state solution is going to be analyzed for the finite domain and the non-reflective boundaries are going to be derived.

3.2. Transient state solution of the finite rod on elastic foundation with constant stiffness

As has been discussed earlier the system with smoothly varying external stiffness will not be solved analytically, instead the Finite Difference Method will be used to approximate the second order derivative with respect to space. Although this is the case, in order to observe the behaviour due to the change in stiffness the transient solution must be derived. To do this, another method of solving the governing equation has to be used, namely Laplace Transform. First, the way the system is divided into domains has to be changed.

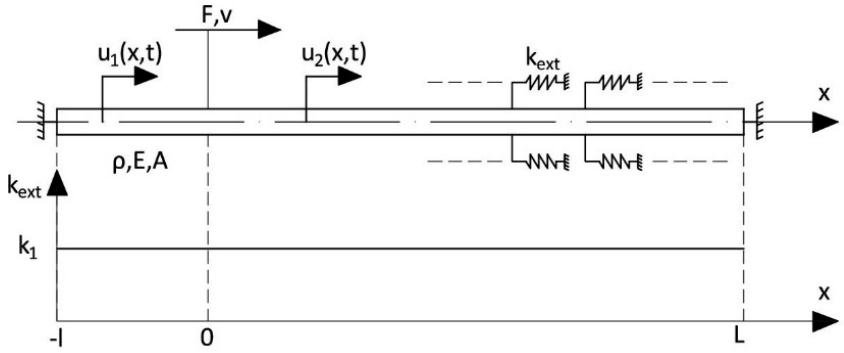

Figure 5 - Finite rod on elastic foundation with constant stiffness subjected to a uniformly moving constant load

For this case, the reference frame is fixed and the two domains are as follows: domain 1 for $x=(-l,0)$ and domain 2 for $x=(0,L)$. The load is entering the computational domain at $x=0$. For this method, it is more convenient to introduce the forcing into the equations of motion and not in the interface conditions. Thus, the equations of motion read:

$$\ddot{u}_1 - c^2 u_1'' + \omega_0^2 u_1 = 0 \qquad \text{for } x=(-l,0) \tag{23}$$

$$\ddot{u}_2 - c^2 u_2'' + \omega_0^2 u_2 = \frac{F_0}{\rho A}\delta(x-vt)\left(H(t)-H\left(t-\frac{L}{v}\right)\right) \qquad \text{for } x=(0,L) \tag{24}$$

- δ and H represent the Dirac-delta function and the Heaviside-step function, respectively

If the system is analyzed for time moments between $0 \le t \le \frac{L}{v}$, then the Heaviside-step function reduces to *1* and the equation simplifies to:

$$\ddot{u}_2 - c^2 u_2'' + \omega_0^2 u_2 = \frac{F_0}{\rho A}\delta(x-vt) \tag{25}$$

The interface and boundary conditions, respectively, read:

$$u_1 = u_2 \qquad \text{at } x=0 \tag{26}$$

$$u_1' = u_2' \qquad \text{at } x=0 \tag{27}$$

$$-c^2 u_1' + \varepsilon_{B,-l}\dot{u}_1 = 0 \qquad \text{at } x = -l \tag{28}$$

$$c^2 u_2' + \varepsilon_{B,L}\dot{u}_2 = 0 \qquad \text{at } x = L \tag{29}$$

The Forward Laplace transform and Inverse Laplace transform, respectively, are defined as:

$$\tilde{u}(x,s) = \int_0^\infty u(x,t)\cdot e^{-st}\,dt \tag{30}$$

$$u(x,t) = \frac{1}{2\pi i}\lim_{\omega\to\infty}\int_{\sigma-i\omega}^{\sigma+i\omega} \tilde{u}(x,s)\cdot e^{st}\,ds \tag{31}$$

- $s = \sigma + i\omega$ represents the complex Laplace variable

It is important to note that for $s = i\omega$ the Inverse Laplace transform simplifies to:

$$u(x,t) = \frac{1}{2\pi}\int_{-\infty}^{\infty} \tilde{u}(x,\omega)\cdot e^{i\omega t}\,d\omega \tag{32}$$

Performing the forward Laplace transform over time to the equations of motion, eq. (23) and (24), the boundary and interface conditions, eq. (26) – (29), the governing equation in the Laplace domain is obtained, eq. (33) - (38).

$$\tilde{u}_1'' + R^2\tilde{u}_1 = -\frac{1}{c^2}\left(s u_1(t=0) + \dot{u}_1(t=0)\right) \qquad \text{for } x = (-l, 0) \tag{33}$$

$$\tilde{u}_2'' + R^2\tilde{u}_2 = -\frac{1}{c^2}\left(s u_2(t=0) + \dot{u}_2(t=0) + \frac{F_0}{\rho A}\frac{1}{v}e^{-\frac{s}{v}x}\right) \text{ for } x = (0, L) \tag{34}$$

$$\tilde{u}_1 = \tilde{u}_2 \qquad \text{at } x = 0 \tag{35}$$

$$\tilde{u}_1' = \tilde{u}_2' \qquad \text{at } x = 0 \tag{36}$$

$$-c^2\tilde{u}_1' + s\varepsilon_{B,-l}\tilde{u}_1 - \varepsilon_{B,-l}u_1(t=0) = 0 \qquad \text{at } x = -l \tag{37}$$

$$c^2\tilde{u}_2' + s\varepsilon_{B,L}\tilde{u}_2 - \varepsilon_{B,L}u_2(t=0) = 0 \qquad \text{at } x = L \tag{38}$$

- $R = \dfrac{\sqrt{-s^2-\omega_0^2}}{c}$ is the wavenumber and the definition of the branches is discussed in eq. (44)
- $u_{1,2}(t=0)$, $\dot{u}_{1,2}(t=0)$ represent the initial displacement and initial velocity, respectively

It must be noted that by applying the Laplace transform the equations of motion became ordinary second order differential equations which are more straightforward to solve than the partial second order differential equations, from the time domain.

3.2.1. Trivial initial conditions

In order to observe the transient motion, it is constructive to first choose trivial initial conditions. This is equivalent to the domain being at rest when the load enters, which is expected to produce transient motion and waves propagating through the rod.

The solutions to the homogeneous equations of motion, eq. (23) and (24) with trivial initial conditions and without the right-hand side, read:

$$\tilde{u}_{1,\text{hom}}(x,s) = C_1 \cdot e^{-iRx} + C_2 \cdot e^{iRx} \qquad \text{for } x = (-l, 0) \tag{39}$$

$$\tilde{u}_{2,\text{hom}}(x,s) = C_3 \cdot e^{-iRx} + C_4 \cdot e^{iRx} \qquad \text{for } x = (0, L) \tag{40}$$

The particular solution to the second domain is going to be sought for assuming the same form as the load: $\tilde{u}_{2,part}(x,s) = Ae^{-\frac{s}{v}x}$. By substituting it in the inhomogeneous equation of motion of the second domain, eq. (34), the particular amplitude is found and consequently, the whole particular solution. The right-hand side of eq. (41) is obtained after some manipulations.

$$\tilde{u}_{2,part}(x,s) = -\frac{F_0}{\rho A c^2}\frac{1}{v}\frac{1}{\frac{s^2}{v^2} + R^2}e^{-\frac{s}{v}x} = -\frac{F_0}{\rho A}\frac{\beta^2}{\omega_0^2}\frac{v}{s^2 - \beta^2 v^2}e^{-\frac{s}{v}x} \tag{41}$$

The general solutions to the equations of motion, eq. (33) and (34), now read:

$$\tilde{u}_1(x,s) = C_1 \cdot e^{-iRx} + C_2 \cdot e^{iRx} \tag{42}$$

$$\tilde{u}_2(x,s) = C_3 \cdot e^{-iRx} + C_4 \cdot e^{iRx} - \frac{F_0}{\rho A}\frac{\beta^2}{\omega_0^2}\frac{v}{s^2 - \beta^2 v^2}e^{-\frac{s}{v}x} \tag{43}$$

One should realize that s is a variable and by anticipating that eventually it is going to be chosen as $s = i\omega$, with ω going from $-\infty$ to ∞, the wavenumber becomes:

$$R = \frac{\sqrt{\omega^2 - \omega_0^2}}{c}$$

For certain values of ω, the complex radical will have points of sign change, which are called branch points. These have to be formally defined. Considering that the cut-off frequency is always positive, $\omega_0 > 0$, the branches of the complex radicals are defined as:

$$\sqrt{\omega^2 - \omega_0^2} = \begin{cases} -\sqrt{\omega^2 - \omega_0^2}, & \omega < -\omega_0 \\ -i\sqrt{\omega_0^2 - \omega^2}, & \omega^2 \le \omega_0^2 \\ \sqrt{\omega^2 - \omega_0^2}, & \omega > \omega_0 \end{cases} \tag{44}$$

The next two figures help visualize the meaning of the general solutions (42), (43) and how the branch points influence them.

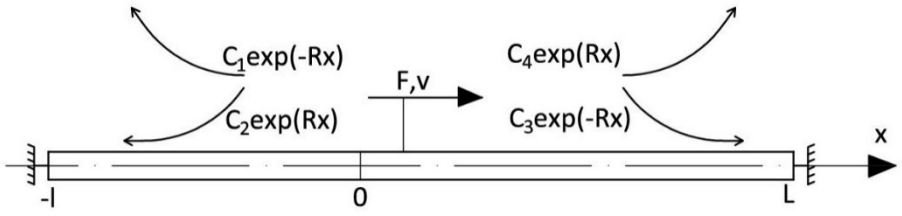

Figure 6 - Rod on elastic foundation with constant stiffness, visualizing the four type of displacements present in the solution for $\omega^2 \leq \omega_0^2$

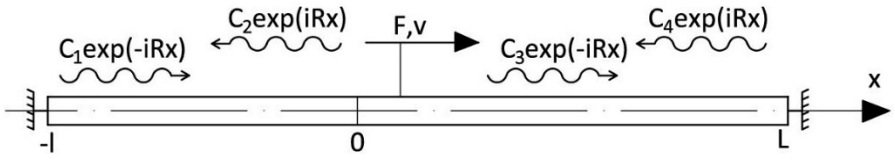

Figure 7- Rod on elastic foundation with constant stiffness, visualizing the four type of propagating waves present in the solution for $\omega > \omega_0$

At this point it should be explained why the system has been divided in these two domains and the load entering at $t = 0$ directly at $x = 0$. If the system would have only one domain, namely $x = (0, L)$, it would also have only one solution with two waves propagating (for $\omega > \omega_0$) through the rod. In order to find the two non-reflective boundaries, it should be imposed that the amplitudes of both waves are zero. This would mean that, although the system is at rest before the load enters the domain, it would still not excite any transients. This is, of course, non-sense. That is why the extra domain is included, $x = (-l, 0)$, to permit waves to propagate away from the load towards the boundaries, but not permit waves to propagate backwards from the boundaries to the load, thus finding the non-reflective boundaries. Note that this domain can be very small, but not zero.

In order to proceed and find the non-reflective boundary coefficients, the general solutions, eq. (42) and (43), are substituted in the boundary conditions (37) and (38), keeping in mind that the initial displacement present in the boundary condition is zero due to trivial initial conditions. The following equations are obtained:

$$C_1 = \frac{ic^2 R - s\varepsilon_{B,-l}}{ic^2 R + s\varepsilon_{B,-l}} C_2 e^{-2iRl} \tag{45}$$

$$C_4 = \underbrace{\frac{ic^2 R - s\varepsilon_{B,L}}{ic^2 R + s\varepsilon_{B,L}} C_3 e^{-2iRL}}_{\text{waves reflecting from the boundary at } x = L} + \underbrace{\frac{s\left(v\varepsilon_{B,L} - c^2\right)}{ic^2 R + s\varepsilon_{B,L}} \frac{F_0}{\rho A} \frac{\beta^2}{\omega_0^2} \frac{1}{s^2 - \beta^2 v^2} e^{-\left(iR + \frac{s}{v}\right)L}}_{\text{waves due to the removal of the load at } x = L} \tag{46}$$

The expression for the waves traveling backwards from the boundary at $x = L$ is now composed of two contributors, the reflected waves at the boundary and the waves generated due to the load exiting the computational domain. The second contributor was not present in the previous cases because the steady-state solution does not encompass these transients. Although it is reasonable to expect transient disturbance due to the load exiting the domain, it does not accurately represent the infinite system, where the load is always present in the infinite domain. Moreover, from eq. (46) it is not possible to find one unique $\varepsilon_{B,L}$ for which no transients are induced at the right boundary. To overcome this problem, there are two solutions, both of them involve changing the system. The first one is to change the finite system into a semi-infinite system in such a way that the load cannot exit the domain. The second solution is more pragmatic, by applying a type of forcing at $x = L$ boundary exactly when the forcing exits the domain, in such a way that it cancels the transients induced by it. This forcing, in the Laplace domain, is exactly the expression corresponding to the removal of the load from eq. (46), but with opposite sign. The first solution is chosen further.

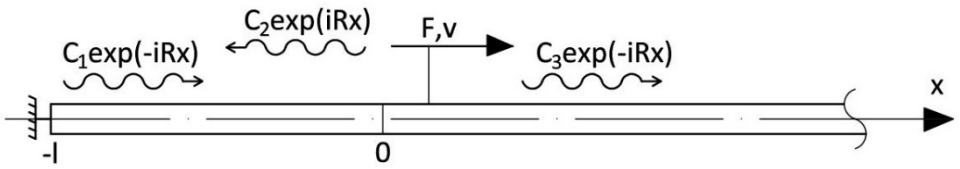

Figure 8 – Semi-infinite rod on elastic foundation with constant stiffness, visualizing the three type of propagating waves present in the solution for $\omega > \omega_0$

The governing equation changes, but not significantly. The boundary condition, eq. (29) and subsequently eq. (38), are replaced by the radiation condition, meaning that the constant $C_4 = 0$, thus the terms related to this constant turn to zero.

The non-reflective boundary coefficient at $x = -l$ can be found from equation (45).

$$\varepsilon_{B,-l} = \frac{iRc^2}{s} \xrightarrow{s=i\omega} \varepsilon_{B,-l} = \frac{c\sqrt{\omega^2 - \omega_0^2}}{\omega} \tag{47}$$

It must be noted that this expression for the non-reflective boundary is in the Laplace domain. The difference is that in the time domain, a physically real dashpot would only be non-reflective for one specific frequency. Due to the sudden impact at the load entry, waves at all frequencies are being generated, consequently the non-reflective boundary is frequency dependent.

In order to proceed, the displacements, eq. (42), (43), bearing in mind that $C_1 = C_4 = 0$, are substituted in the interface conditions, eq. (35), (36). Solving the system of two algebraic equations for the two unknowns C_2, C_3, the displacements in Laplace domain to the two domains have been found.

$$\tilde{u}_1(x,s) = -\frac{1}{2}\frac{F_0}{\rho A}\frac{\beta^2}{\omega_0^2}\frac{i(s-iRv)}{R(s^2-\beta^2v^2)}\cdot e^{iRx} \tag{48}$$

$$\tilde{u}_2(x,s) = -\frac{1}{2}\frac{F_0}{\rho A}\frac{\beta^2}{\omega_0^2}\frac{i(s+iRv)}{R(s^2-\beta^2v^2)}\cdot e^{-iRx} - \frac{F_0}{\rho A}\frac{\beta^2}{\omega_0^2}\frac{v}{s^2-\beta^2v^2}e^{-\frac{s}{v}x} \tag{49}$$

In order to visualize this transient motion of the system, these expressions have to be taken back to the time domain using the inverse Laplace transform. If $s = i\omega$ is assumed, the expressions for the displacements, eq. (48) and (49) become:

$$\tilde{u}_1(x,\omega) = -\frac{1}{2}\frac{F_0}{\rho A}\frac{\beta^2}{\omega_0^2}\frac{(\omega-Rv)}{R(\omega^2+\beta^2v^2)}\cdot e^{iRx} \tag{50}$$

$$\tilde{u}_2(x,s) = -\frac{1}{2}\frac{F_0}{\rho A}\frac{\beta^2}{\omega_0^2}\frac{(\omega+Rv)}{R(\omega^2+\beta^2v^2)}\cdot e^{-iRx} - \frac{F_0}{\rho A}\frac{\beta^2}{\omega_0^2}\frac{v}{\omega^2+\beta^2v^2}e^{-i\frac{\omega}{v}x} \tag{51}$$

- $R = \dfrac{\sqrt{\omega^2-\omega_0^2}}{c}$ and the complex radical is defined as in eq. (44)

It can be observed that there is no real valued frequency for which the expressions (50) and (51) have poles (division by 0). Therefore, because the integration has to be done, in the complex plane, at the right of all the poles, choosing $s = i\omega$ satisfies this criterion.

The analytical procedure of taking the inverse Laplace transform is very difficult, if not impossible, due to the wavenumber being present both in the numerator as in the denominator, which contains the square root of the frequency, which is the variable of integration. Consequently, the inverse Laplace transform is going to be performed numerically, by truncating the limits of the integrals (52) and (53) and approximating them. In this additional thesis, the trapezoidal rule is used for the approximation of the integrals. To obtain more accurate results, more sophisticated algorithms can be used.

$$u_1(x,t) = \frac{1}{2\pi}\int_{-\infty}^{\infty}\tilde{u}_1(x,\omega)\cdot e^{i\omega t}d\omega \tag{52}$$

$$u_2(x,t) = \frac{1}{2\pi}\int_{-\infty}^{\infty}\tilde{u}_2(x,\omega)\cdot e^{i\omega t}d\omega \tag{53}$$

To make sure that the solution converges, a small amount of damping is added to the system. The changed expressions are derived in Annex A.

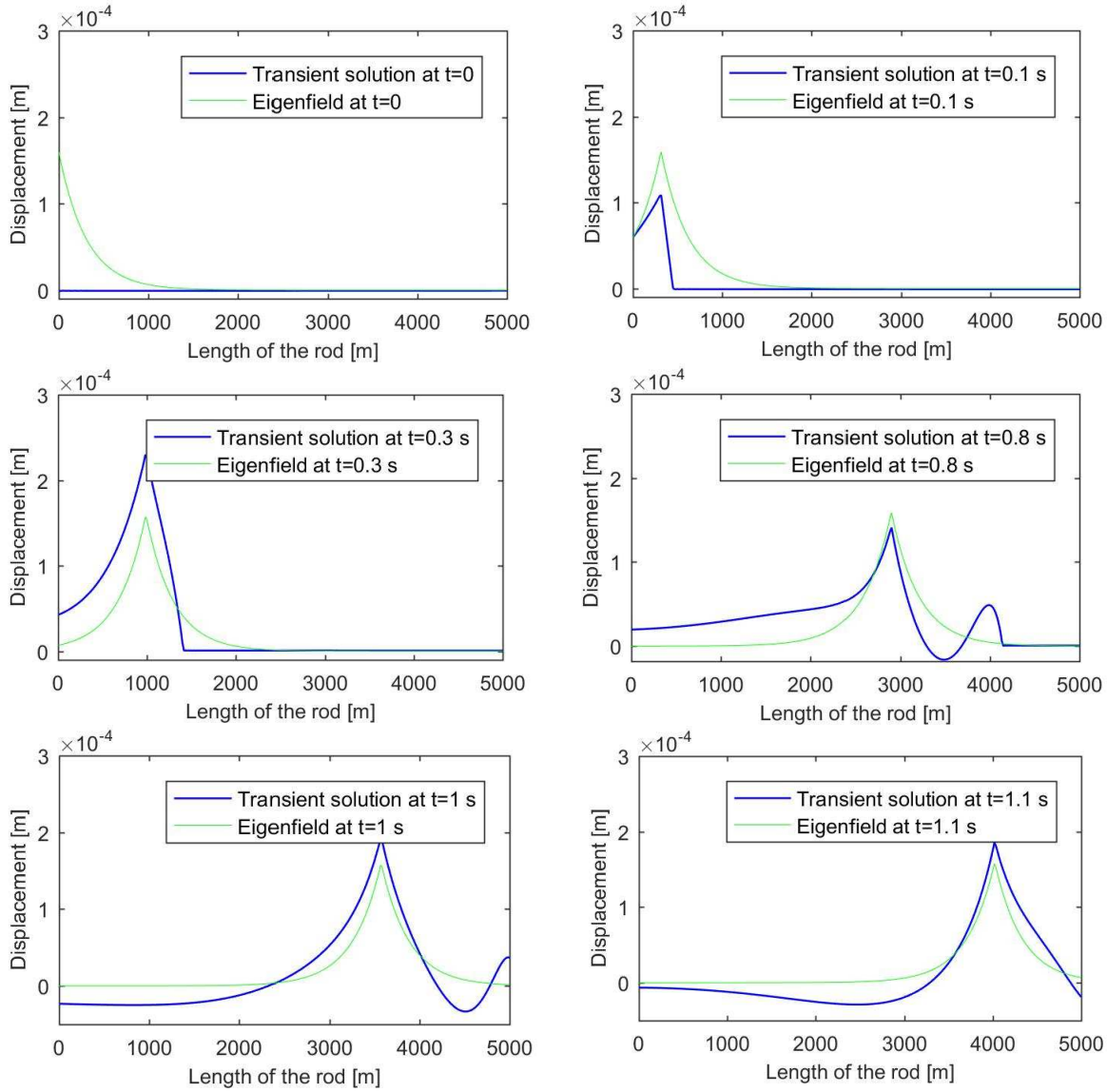

Figure 9 - Transient solution with trivial initial conditions, v = 0.7 c

In Figure 9, in the upper left plot it can be seen that the computational domain is at rest when the load enters the domain. The displacements develop in the next figures and then in the middle right figure the waves propagating towards the right boundary can be clearly seen. The wave front is indistinguishable before this time moment because the velocity of the load is close to the velocity of the waves. Finally, in the last two figures the wave front reaches the right boundary, but it doesn't get reflected, meaning that the non-reflective coefficient is correct.

3.2.2. Initial conditions chosen such that no transients are excited

In order to truly simulate the behaviour of the infinite system, the transients generated by the load entering the domain should be inexistent. Thus, the initial conditions should be chosen such that immediately after entering, the steady-state eigenfield is developed. These initial conditions are exactly those from the steady-state solution, taking the time derivative to find the initial velocity and evaluating them at $t = 0$.

$$u_1(x, t=0) = \frac{1}{2}\frac{F_0}{\rho A}\frac{\beta}{\omega_0^2}e^{\beta x} \quad , \qquad \dot{u}_1(x, t=0) = -\frac{1}{2}\frac{F_0}{\rho A}\frac{\beta^2 v}{\omega_0^2}e^{\beta x} \tag{54}$$

$$u_2(x, t=0) = \frac{1}{2}\frac{F_0}{\rho A}\frac{\beta}{\omega_0^2}e^{-\beta x} \quad , \qquad \dot{u}_2(x, t=0) = \frac{1}{2}\frac{F_0}{\rho A}\frac{\beta^2 v}{\omega_0^2}e^{-\beta x} \tag{55}$$

Substituting the initial conditions, eq. (54) and (55), into the equations of motion for the semi-infinite system in Laplace domain, eq. (33) and (34), and after performing some trivial manipulations they become:

$$\tilde{u}_1'' + R^2\tilde{u}_1 = -\frac{1}{2}\frac{F_0}{\rho A c^2}\frac{\beta}{\omega_0^2}(s - \beta v)e^{\beta x} \qquad \text{for } x = (-l, 0)$$

$$\tilde{u}_2'' + R^2\tilde{u}_2 = -\frac{1}{2}\frac{F_0}{\rho A c^2}\frac{\beta}{\omega_0^2}(s + \beta v)e^{-\beta x} - \frac{F_0}{\rho A c^2}\frac{1}{v}e^{-\frac{s}{v}x} \qquad \text{for } x = (0, L)$$

After deriving the particular solutions as we did in the previous chapter, by assuming the same form as the force, the general solution become:

$$\tilde{u}_1(x, s) = C_1 \cdot e^{-iRx} + C_2 \cdot e^{iRx} + \frac{1}{2}\frac{F_0}{\rho A}\frac{\beta}{\omega_0^2}\frac{1}{s + \beta v}e^{\beta x} \tag{56}$$

$$\tilde{u}_2(x, s) = \underbrace{C_3 \cdot e^{-iRx}}_{\text{transients}} + \underbrace{\frac{1}{2}\frac{F_0}{\rho A}\frac{\beta}{\omega_0^2}\frac{1}{s - \beta v}e^{-\beta x}}_{\text{initial state}} - \underbrace{\frac{F_0}{\rho A}\frac{\beta^2}{\omega_0^2}\frac{v}{s^2 - \beta^2 v^2}e^{-\frac{s}{v}x}}_{\text{forcing}} \tag{57}$$

steady-state eigenfield

The forcing term and the initial state term together give the steady-state eigenfield, because the forcing alone produces transients, as it has been seen in the previous case.

The question arises now, how should the non-reflective boundary be sought for? Under the form of a spring or a dashpot? Provided that the initial conditions have been chosen correctly, they should ensure that no transients are generated by the load entry, while the non-reflective boundary should ensure that the eigenfield interaction with the boundary does not generate transients. This leads to the steady-state which doesn't have a propagation behaviour. Thus, the non-reflective boundary will be searched for as a spring.

The interface conditions are the same, eq. (35) and (36), while the boundary condition becomes:

$$-c^2\tilde{u}_1' + k_{B,-l}\tilde{u}_1 = 0 \qquad \text{at } x = -l \tag{58}$$

Substituting the displacements, eq. (56) and (57), into the boundary condition, eq. (58), and interface conditions, eq. (35) and (36), and solving the system of equations, the three unknowns C_1, C_2, C_3 are found:

$$C_1 = C_3 = -\frac{1}{2}\frac{F_0}{\rho A}\frac{\beta}{\omega_0^2}\frac{1}{s+\beta v}\frac{k_{B,-l}-\beta c^2}{k_{B,-l}+iRc^2}e^{-(iR+\beta)l} \tag{59}$$

$$C_2 = 0 \tag{60}$$

From Figure 8, it is clear that in order to find the non-reflective boundary, the sufficient condition is that the constant $C_1 = 0$ and by doing so all the constants relating to the transients become zero. This is no surprise because by choosing the right initial conditions no transient motion should be generated. The non-reflective boundary coefficient reads:

$$k_{B,-l} = \beta c^2 \tag{61}$$

This effectively shows that no transients are being excited by the load entry, thus exhibiting the same behaviour as the steady-state solution with the advantage that, by using Laplace Transform, it can also encompass the eventual transients generated by the varying external stiffness.

The displacement expressions now read:

$$\tilde{u}_1(x,s) = \frac{1}{2}\frac{F_0}{\rho A}\frac{\beta}{\omega_0^2}\frac{1}{s+\beta v}e^{\beta x} \tag{62}$$

$$\tilde{u}_2(x,s) = \frac{1}{2}\frac{F_0}{\rho A}\frac{\beta}{\omega_0^2}\frac{1}{s-\beta v}e^{-\beta x} - \frac{F_0}{\rho A}\frac{\beta^2}{\omega_0^2}\frac{v}{s^2-\beta^2 v^2}e^{-\frac{s}{v}x} \tag{63}$$

In this case, the inverse Laplace transform can be performed analytically, obtaining the following expressions:

$$u_1(x,t) = \frac{1}{2}\frac{F_0}{\rho A}\frac{\beta}{\omega_0^2}e^{\beta(x-vt)} \tag{64}$$

$$u_2(x,t) = \frac{1}{2}\frac{F_0}{\rho A}\frac{\beta}{\omega_0^2}\left(e^{-\beta(x-vt)} - 2H\left(t-\frac{x}{v}\right)\sinh\left(\beta(vt-x)\right)\right) \tag{65}$$

contributor 1 *contributor 2*

- H represents the Heaviside-step function

To understand why this represents the steady-state eigenfield, the two contributors in the second solution have to be visualized.

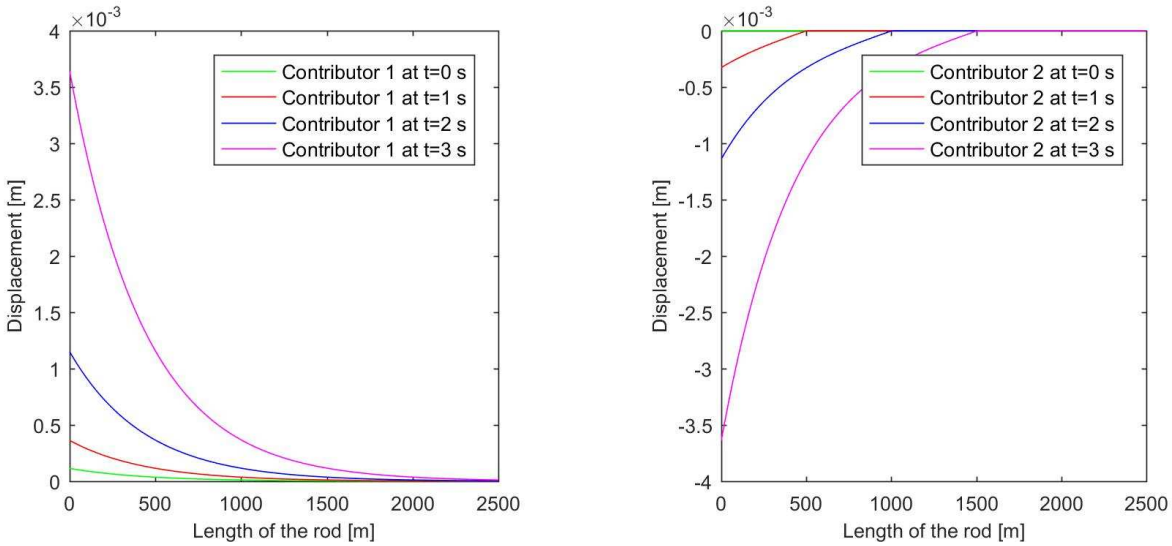

Figure 10 - The two contributors from the solution of the second domain plotted for different time moments

It can be seen from the above figures that the first contributor alone will lead to infinite displacements and there is no eigenfield moving along with the load. Meanwhile, the second contributor, due to the Heaviside-step function, only acts behind the load, canceling the infinitely increasing displacements of the first contributor. Thus, adding the two contributors and including the solution of the first domain, the eigenfield is obtained as seen in Fig. 11.

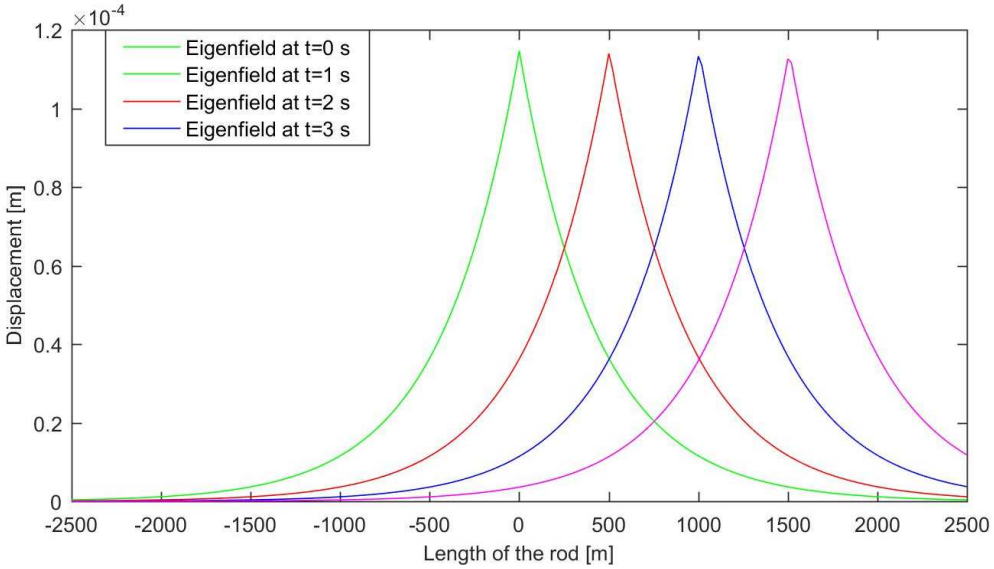

Figure 11 - Solutions for both domains plotted together for different time moments

It has been mentioned that although this represents the steady-state eigenfield for the system with constant external stiffness, because it was solved with the Laplace transform, this method encompasses the eventual transients generated by an eventual change in external stiffness. The only problem left now is to deal with the reflection of the generated transients (due to the change in stiffness) at the boundaries. The non-reflective boundary eq. (61) is non-reflective only for the non-propagating eigenfield, it does not absorb the propagating waves. In the next subchapter, this issue is going to be addressed.

3.2.3. Including in the solution a wave traveling from the stiffness transition

Although all the expressions have been derived for the system with constant stiffness, it is possible to artificially add a propagating (for $\omega > \omega_0$) wave in the solution for the second domain, eq. (57), which represents a wave propagating from the stiffness change. This is done in order to find a non-reflective boundary for both the propagating wave as well as for the eigenfield. By doing so, the eq. (57) changes to:

$$\tilde{u}_2(x,s) = C_3 \cdot e^{-iRx} + W \cdot e^{iRx} + \frac{1}{2}\frac{F_0}{\rho A}\frac{\beta}{\omega_0^2}\frac{1}{s-\beta v}e^{-\beta x} - \frac{F_0}{\rho A}\frac{\beta^2}{\omega_0^2}\frac{v}{s^2-\beta^2 v^2}e^{-\frac{s}{v}x} \tag{66}$$

- W represents the random amplitude of the wave generated by the change in stiffness

The next figure helps visualize the new system.

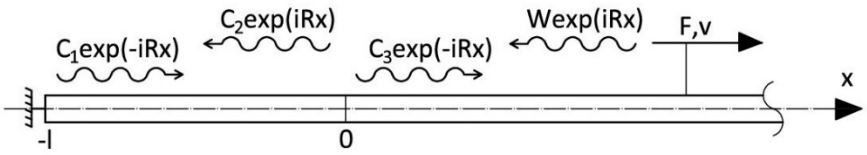

Figure 12 - Semi-infinite rod on elastic foundation after load has crossed the stiffness change, visualizing the four type of propagating waves present in the solution for $\omega > \omega_0$

Once more, the question of how should the non-reflective boundary be sought for arises. It has been seen in the previous subchapters that in order to suppress the non-propagating eigenfield the boundary coefficient turns out to be a spring and in the case of propagating waves it is a dash-pot. Thus, it comes as a natural extension that the non-reflective boundary for both eigenfield and propagating waves should be a combination of both a spring and a dash-pot. The two elements are combined in parallel, as seen in the figure below. This type of boundary element is called a Kelvin-Voigt element.

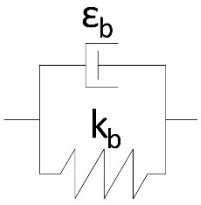

Figure 13 - Kelvin-Voigt element

The boundary condition, eq. (37), becomes:

$$-c^2\tilde{u}_1' + \left(s\varepsilon_{B,-l} + k_{B,-l}\right)\tilde{u}_1 - \varepsilon_{B,-l}\underbrace{u_1(t=0)}_{\text{initial displacement}} = 0 \qquad \text{at } x = -l \tag{67}$$

Note that the initial displacement is present in the boundary condition, but only for the dash-pot, due to its proportionality with velocity.

The interface conditions, eq. (35), (36) and the solution for the first domain, eq. (56), are the same. Substituting the two solutions, eq. (56) and (66), into the boundary and interface conditions, eq. (66), (35) and (36), and solving the system of equations, the three unknowns C_1, C_2, C_3 are found, eq. (68) and (69). Note that W is not an unknown, it is just an assumed amplitude for the backwards propagating wave excited by the change in external stiffness.

$$C_2 = W \tag{68}$$

$$C_1 = C_3 = \underbrace{-W \frac{iRc^2 - s\varepsilon_{B,-l} - k_{B,-l}}{iRc^2 + s\varepsilon_{B,-l} + k_{B,-l}} e^{-2iRl}}_{\text{Contribution from the backward propagating wave due to change in stiffness}} + \underbrace{\frac{1}{2}\frac{F_0}{\rho A}\frac{\beta}{\omega_0^2}\frac{\beta c^2 + \beta v\varepsilon_{B,-l} - k_{B,-l}}{\left(iRc^2 + s\varepsilon_{B,-l} + k_{B,-l}\right)\left(s+\beta v\right)} e^{-(iR+\beta)l}}_{\text{Contribution from the eigenfield interaction with the boundary}} \tag{69}$$

It makes sense that constant $C_2 = W$ because due to the chosen initial state, there are no other transients present in the rod except the one introduced 'artificially' to represent the disturbances produced at the stiffness change.

The constant C_1 represents the reflections at the boundary $x = -l$. It can be seen from expression (69) that it has two contributions. One of the contributions is from the eigenfield that interacts with the boundary, which was present in the previous case where there was no wave propagating from the stiffness change (see subchapter 3.3.2). It can be observed that for $W = 0$ and $\varepsilon_{B,-l} = 0$, which represents the previous case, the same non-reflective boundary condition is obtained, $k_{B,-l} = \beta c^2$. The other contribution is represented by the backward traveling wave excited by the load traveling over the stiffness change. This contributor was present in the transient case with trivial initial conditions (see subchapter 3.3.1), where the eigenfield was not yet developed and the only perturbations present in the rod were the propagating waves. Once again, expressing this limit case by canceling the contribution from the eigenfield and by considering $k_{B,-l} = 0$, the same non-reflective boundary coefficient is found, $\varepsilon_{B,-l} = \frac{ic^2 R}{s}$.

In order to find the non-reflective boundary for both contributions, they have to be set to zero independently, forming the following system of equations:

$$iRc^2 - s\varepsilon_{B,-l} - k_{B,-l} = 0 \tag{70}$$

$$\beta c^2 + \beta v\varepsilon_{B,-l} - k_{B,-l} = 0 \tag{71}$$

Solving the system of equations, the boundary coefficients, $k_{B,-l}$ and $\varepsilon_{B,-l}$, are found.

$$k_{B,-l} = \frac{\beta c^2\left(iRv + s\right)}{\beta v + s} \quad , \qquad \varepsilon_{B,-l} = \frac{c^2\left(iR - \beta\right)}{\beta v + s} \tag{72}$$

Because these are not ordinary boundary coefficients, it has to be checked if by implementing them it doesn't lead to an unstable system, or in other words, an ill posed initial boundary value problem. By assuming $s = i\omega$ and plotting the two expressions, eq. (72), with respect to frequency, the following plots are obtained:

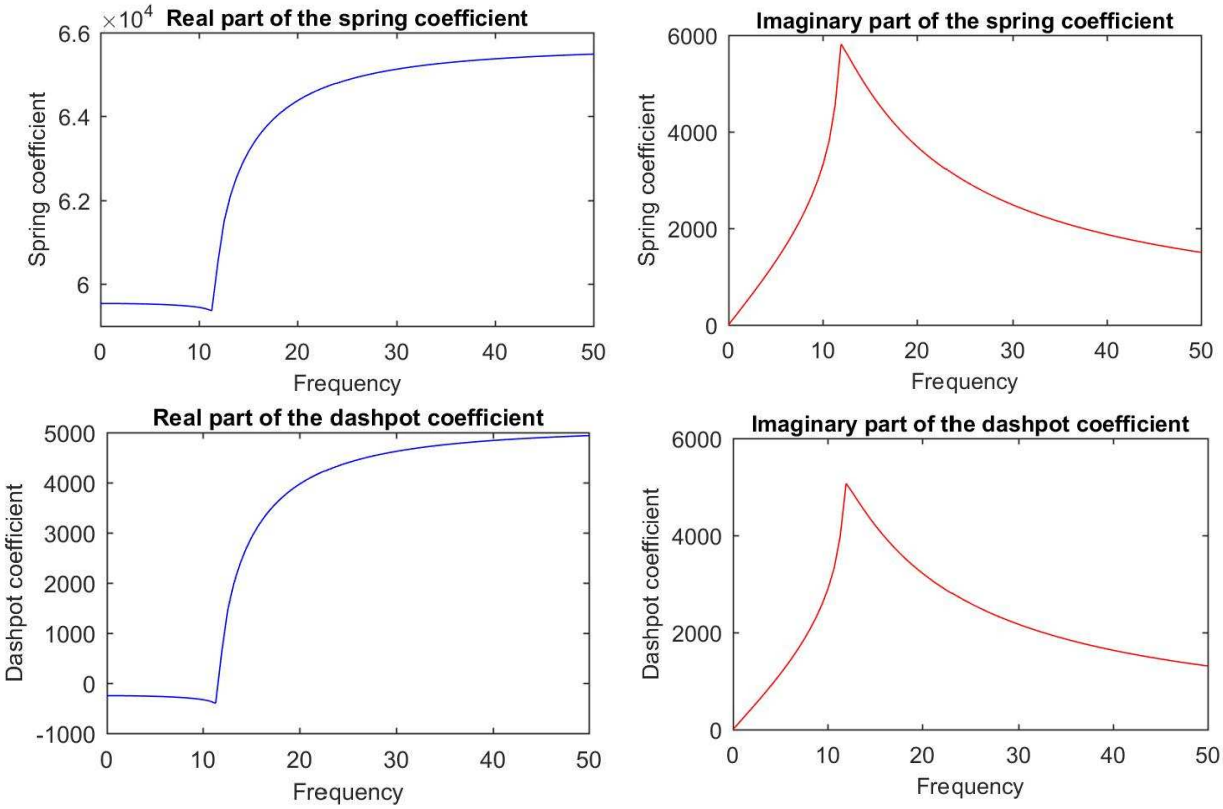

Figure 14 - Plots of the real and imaginary parts of the two non-reflective boundary coefficients

From Figure 14 it can be observed that the real parts of the two coefficients tend to some constant values as the frequency tends to infinity. The coefficients can now be split up into a decaying function with respect to frequency and a constant value. The decaying function is called a memory function or relaxation function.

$$k_{B,-l} = f_{k,\infty} + g_k(\omega) \tag{73}$$

$$\varepsilon_{B,-l} = f_{\varepsilon,\infty} + g_\varepsilon(\omega) \tag{74}$$

To find these constant values the limit of the coefficients is taken.

$$f_{k,\infty} = \lim_{\omega\to\infty}\left(\mathrm{Re}\left\{k_{B,-l}\right\}\right) = \beta c(c+v) \tag{75}$$

$$f_{\varepsilon,\infty} = \lim_{\omega\to\infty}\left(\mathrm{Re}\left\{\varepsilon_{B,-l}\right\}\right) = c \tag{76}$$

The memory functions can be found now to be:

$$g_k(\omega) = \frac{\beta c^2 (iRv + s)}{\beta v + s} - \beta c(c + v) \tag{77}$$

$$g_\varepsilon(\omega) = \frac{c^2 (iR - \beta)}{\beta v + s} - c \tag{78}$$

Taking these expressions, eq. (77) and (78), to the time domain by applying the inverse Laplace transform yields complicated expressions, consequently only the plots are going to be presented.

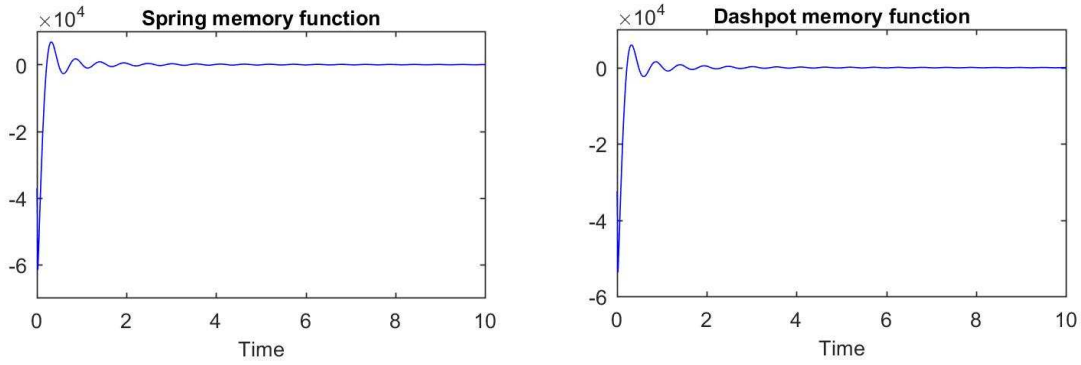

Figure 15 - Memory functions of the two boundary coefficients in the time domain

As admissibility criteria for the boundary coefficients, in the literature there are different requirements for the memory function. Some of them require that the memory function is positive and monotonically decaying [see Kampas 2007]. Although this is not the case, because the memory functions of the boundary coefficients found enclose a finite area on the graph it can be argued that the functions are casual and will not create instability. Also, the behaviour seen in Figure 15 is expected just from looking at the coefficients, eq. (72). Both expressions have poles at $s = -\beta v$ which represents the exponentially decaying behaviour, while the wavenumber's branch points at $s = \pm i\omega_0$ account for the oscillatory character. Moreover, as it will be seen later (chapter 5), using these boundary coefficients in the model does not lead to unstable behaviour in none of the cases studied.

It must also be noticed that the two coefficients can be added together to form a single dynamical boundary. The following boundary condition is employed:

$$\pm c^2 \tilde{u}' + \underbrace{(s\varepsilon_B + k_B)}_{k_{dyn}} \tilde{u} - \varepsilon_B u(t=0) = 0$$

$$k_{dyn} = s\varepsilon_B + k_B = iRc^2$$

This expression represents the general non-reflective boundary condition, also found in the transient case with trivial initial conditions, but in this case, it has to be split up in the two parts (spring and dashpot) because the initial displacement is only applied to the dashpot part.

3.3. Overview and concluding remarks of the chapter

Now that the non-reflective boundary coefficients have been found and the initial state is also known, the system with the varying external stiffness can be solved. As discussed previously, the approach of solving this system is to use a numerical method, namely the Finite Difference Method. Due to the numerical analysis, there is no need in our model for the first domain anymore, because the numerical method does exactly that, splits up the model into many, small domains. Also, it is impossible to model the semi-infinite system, consequently the system is going to have a boundary at $x = L$ with the same properties as the one at $x = 0$. To avoid seeing the transients due to the load removal, the time of analysis is going to be bound by $t = \left[0, \frac{L}{v}\right]$.

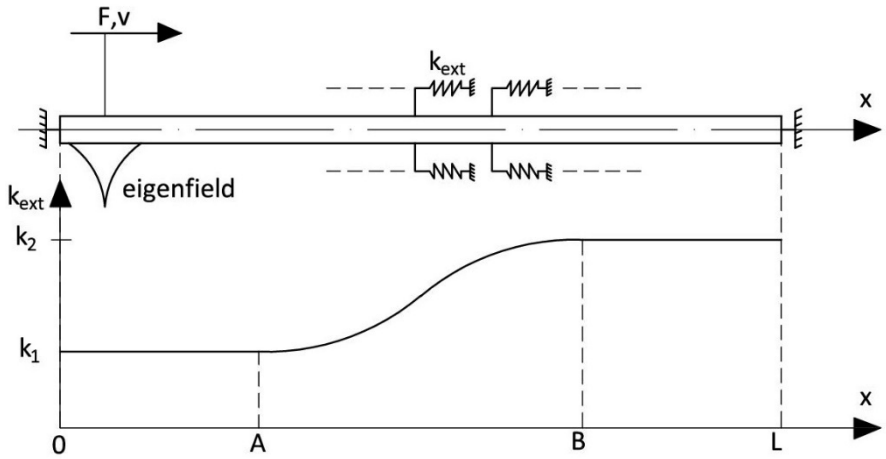

Figure 16 - Finite rod resting on elastic foundation with varying stiffness

Provided that the initial stiffness plateau (see fig. 16 between 0 and A) is long enough that the eigenfield does not already excite transients before the load entry, the initial state of the rod is the same as previously discussed in chapter 3.3.2, eq. (54) and (55). The boundary conditions in the Laplace domain are also the same as discussed previously.

$$-c^2\tilde{u}' + \left(s\varepsilon_{B,0} + k_{B,0}\right)\tilde{u} - \varepsilon_{B,0}u\left(t=0\right) = 0 \qquad \text{at } x = 0 \qquad (79)$$

$$c^2\tilde{u}' + \left(s\varepsilon_{B,L} + k_{B,L}\right)\tilde{u} - \varepsilon_{B,L}u\left(t=0\right) = 0 \qquad \text{at } x = L \qquad (80)$$

The equation of motion in the Laplace domain is the same, except that the cut-off frequency is space dependent.

$$-c^2\tilde{u}'' + \left(s^2 + \omega_0^2\left(x\right)\right)\tilde{u} = su_2\left(t=0\right) + \dot{u}_2\left(t=0\right) + \frac{F_0}{\rho A}\frac{1}{v}e^{-\frac{s}{v}x} \text{ for } x = \left(0, L\right) \qquad (81)$$

Due to the space dependence of the coefficient in the ordinary differential equation, eq. (96), the harmonic solution of the form $u\left(x\right) = Ae^{kx}$ does not work anymore. For this reason, the Finite Difference Method is used to approximate the second order derivative with respect to space by splitting the domain into small elements.

$$u_n'' = \frac{1}{l^2}\left(u_{n-1} - 2u_n + u_{n+1}\right) \tag{82}$$

- $l = \frac{L}{N}$ represents the length of one element, L the length of the rod, N the number of elements

By doing so, the differential equation of motion, eq. (82), changes to a system of N+1 algebraic equations. How the system is solved numerically is discussed in Annex 3 in more detail.

So far, the system from Figure 16 has been solved and modeled.

The time dependence of the system has been solved using the Laplace transform in order to account for the transient motion once the load passes over the stiffness change. The inverse Laplace transform has been applied numerically by evaluating the integral with a trapezoidal rule. In order not to excite any transient motion at the load entry in the computational domain, the initial state has been found. This has been derived based on the steady-state solution of the constant stiffness system, where the external stiffness matches the stiffness of the initial plateau in Figure 16.

In order to simulate the infinite system, non-reflective boundaries have been found. First, the non-reflective coefficients have been found for the transient case with trivial initial conditions, which turned out to be dashpots, due to the propagating behaviour of the displacements induced. Secondly, the non-reflective boundary for the transient state with 'tuned' initial conditions has been found to be a spring, due to the non-propagating behaviour of the eigenfield. Finally, these non-reflective boundaries have been extended to account for both non-propagating eigenfield and for propagating waves due to the change in stiffness, by combining them into a Kelvin-Voigt element. In the following table these coefficients are presented in a concise way.

Type of analysis / Type of boundary	Transient state with trivial initial conditions	Transient state with tuned initial conditions	Transient state with tuned initial conditions and backward propagating wave
Dashpot (Laplace domain)	$\frac{iRc^2}{s}$		
Spring (Laplace domain)		βc^2	
Kelvin – Voigt element (Laplace domain)			$k_B = \frac{c^2\beta\left(iRv+s\right)}{\beta v+s}$ $\varepsilon_B = \frac{c^2\left(iR-\beta\right)}{\beta v+s}$

Table 1 - Non-reflective boundaries for different types of analysis

In the end, the varying stiffness model has been solved using Finite Difference Method. It must be noted that this case with varying stiffness has already been solved analytically (see Wolfert), but this is beyond the scope of this additional thesis. In the next chapter, the challenge of reducing the computational domain as much as possible is addressed.

4. Finding the initial state of the system with varying external stiffness based on the reciprocity theorem

If the computational domain is truncated close to the stiffness change (for example from point A to point B in the figure below) then the initial state cannot be found by means of steady-state analysis because there is no steady-state solution anymore. Waves that travel backwards from the stiffness change have already been excited before the load enters the domain. This can be visualized in the following figure.

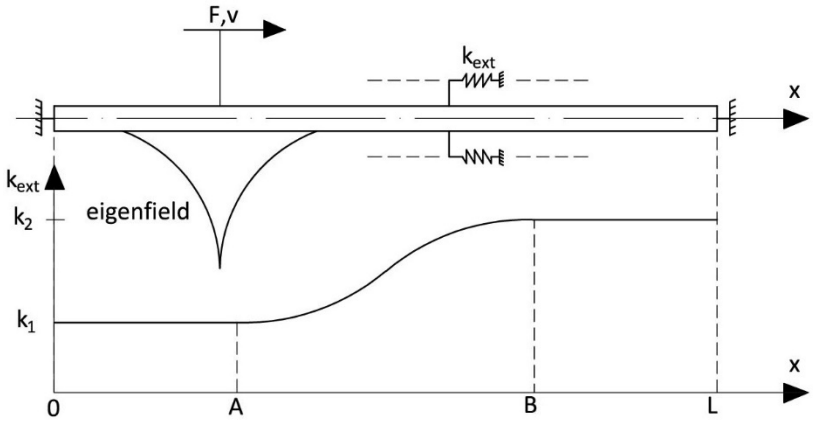

Figure 17 - Finite rod resting on elastic foundation with varying stiffness

This situation requires a different approach, making use of the Reciprocity theorem. In the following paragraphs, the general reciprocity relation is derived. It is important to keep in mind that the purpose of this analysis is to find the initial state, thus all time moments in this analysis are smaller than zero and the load is outside the computational domain.

4.1. The general reciprocity relation

Suppose there are two states, A and B. The equations of motion for the two states are the following:

$$\ddot{u}_A - c^2 u_A'' + \omega_0^2 u_A = \frac{1}{\rho A} q_A \tag{83}$$

$$\ddot{u}_B - c^2 u_B'' + \omega_0^2 u_B = \frac{1}{\rho A} q_B \tag{84}$$

- q_A, q_B represent distributed forces

A time harmonic motion is assumed with the time factor $\exp(i\omega t)$. Replacing it in the equations of motion, they become:

$$\tilde{u}_A'' + k^2 \tilde{u}_A = -\frac{1}{\rho A c^2} \tilde{q}_A \tag{85}$$

$$\tilde{u}_B'' + k^2 \tilde{u}_B = -\frac{1}{\rho A c^2} \tilde{q}_B \tag{86}$$

- $k = \sqrt{\frac{\omega^2 - {\omega_0}^2}{c^2}}$ represent the wavenumber

Note that the 'tilde' notation is used to show the new functions' dependence on only space and not time anymore. Multiplying the equation of motion of each state with the displacement of the other state and subtract one from the other, the local reciprocity relation is obtained:

$$\tilde{u}_A'' \tilde{u}_B - \tilde{u}_B'' \tilde{u}_A = -\frac{1}{\rho A c^2} (\tilde{q}_A \tilde{u}_B - \tilde{q}_B \tilde{u}_A) \tag{87}$$

Integrating this relation over the whole length of the bar yields the general reciprocity relation.

$$\left[\tilde{u}_A' \tilde{u}_B - \tilde{u}_B' \tilde{u}_A \right]_{x=0}^{x=L} = -\frac{1}{\rho A c^2} \int_{x=0}^{x=L} (\tilde{q}_A \tilde{u}_B - \tilde{q}_B \tilde{u}_A) dx \tag{88}$$

Now, the two states can be specified. For state A, the Green's state is chosen. The displacement and the first derivative of it become the Green's function and the first derivative of it, respectively, while the generalized loading becomes the impulse load, as shown in eq. (89).

$$\begin{cases} \tilde{u}_A = \tilde{G} \\ \tilde{u}_A' = \tilde{G}' \\ \tilde{q}_A = \delta(x - x_A) \end{cases} \tag{89}$$

For state B, the actual state is chosen, consequently the functions become:

$$\begin{cases} \tilde{u}_B = \tilde{u} \\ \tilde{u}_B' = \tilde{u}' \\ \tilde{q}_B = 0 \end{cases} \tag{90}$$

The general forcing in the actual state is zero because, as seen in eq. (9), the integration is done over the length of the rod and for the time moments that are analysed ($t \leq 0$), the load is outside the domain.

Expressions (89) and (90) are substituted in the general reciprocity relation, eq. (88), obtaining eq. (91).

$$\left[\tilde{G}'\left(x,x_A,\omega\right)\tilde{u}\left(x,\omega\right)-\tilde{G}\left(x,x_A,\omega\right)\tilde{u}'\left(x,\omega\right)\right]_{x=0}^{x=L}=-\frac{1}{\rho Ac^2}\int_{x=0}^{x=L}\left(\delta\left(x-x_A\right)\tilde{u}\left(x,\omega\right)\right)dx \qquad (91)$$

In the above equation, the integral on the right-hand side is evaluated using the Dirac-delta function property. If the Green's function is split up in two contributions, $\tilde{G}=\tilde{G}_{out}+\tilde{G}_{in}$, it turns out that after it is substituted in eq. (91), the terms relating to $\tilde{G}_{out}$ turn to zero (see Wapenaar,2010). Consequently, relation (91) simplifies to:

$$\tilde{u}_{in}\left(x_A,\omega\right)=-2\rho Ac^2\left[\tilde{G}'\left(x,x_A,\omega\right)\tilde{u}_{in}\left(x,\omega\right)\right]_{x=0}^{x=L} \qquad (92)$$

- subscript *in* stands for inward propagating field and by inward it is meant from the outside the domain to inside the domain

Implementing the non-reflective boundary at $x=L$ will lead to no reflections and consequently no inward propagating field at the right boundary. Eq. (92) simplifies one last time to eq. (93).

$$\tilde{u}_{in}\left(x_A,\omega\right)=2\rho Ac^2\tilde{G}'\left(x=0,x_A,\omega\right)\tilde{u}_{in}\left(x=0,\omega\right) \qquad (93)$$

$\tilde{G}'\left(x=0,x_A,\omega\right)$ represents the first spatial derivative of Green's function measured at $x=0$ due to the Dirac load acting at $x=x_A$. The following figure helps visualize what eq. (108) actually represents.

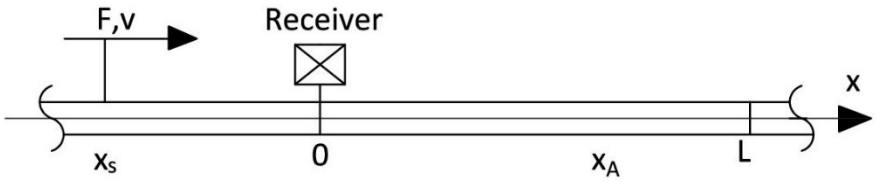

Figure 18 - Visualizing the relation found with the use of reciprocity theorem

The above figure contains the computational domain, $x=\left[0,L\right]$, a receiver exactly at the left boundary and a source of perturbance at x_s. The relation (93) states that the displacement found at any point inside the domain is proportional to the first spatial derivative of the Green's function multiplied with the inwards propagating disturbance field measured by the receiver at $x=0$. The inward propagating disturbance field in our case is exactly the steady-state eigenfield, because at the left of the boundary the external stiffness is constant. The only thing left to do is to find all the Green's functions measured at $x=0$ due to Dirac load acting at $x=x_A$, for the whole computational domain. In the following subchapter, the Green's function is going to be found for the system with constant external stiffness.

4.2. Deriving the Green's function for the system with constant stiffness

The Green's functions are going to be derived for the case with constant stiffness, as a reference for the varying stiffness case, which will be solved numerically. The Green's function represents the response of a system due to an impulse loading. The system is sketched in the following figure.

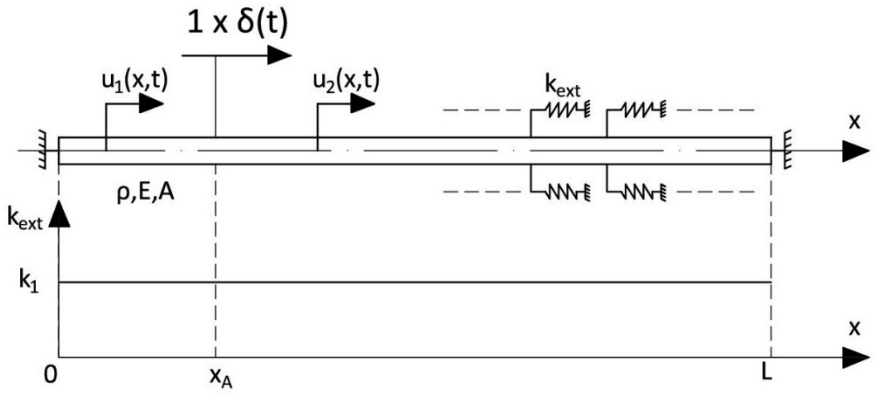

Figure 19 - System for finding the Green's function

The equations of motion are the following:

$$\ddot{u}_1 - c^2 u_1'' + \omega_0^2 u_1 = 0 \qquad \text{for } x < x_A \qquad (94)$$

$$\ddot{u}_2 - c^2 u_2'' + \omega_0^2 u_2 = 0 \qquad \text{for } x > x_A \qquad (95)$$

The interface conditions read:

$$u_1 = u_2 \qquad \text{at } x = x_A \qquad (96)$$

$$u_1' - u_2' = \frac{1}{\rho A c^2} \qquad \text{at } x = x_A \qquad (97)$$

And finally, the boundary conditions:

$$-c^2 u_1' + \varepsilon_{B,0} \dot{u}_1 = 0 \qquad \text{at } x = 0 \qquad (98)$$

$$c^2 u_2' + \varepsilon_{B,L} \dot{u}_2 = 0 \qquad \text{at } x = L \qquad (99)$$

This system is going to be solved by applying the Fourier transform over time and solving the system with respect to space in the frequency domain. Here, Fourier transform is chosen instead of Laplace transform because the domain is at rest at the moment of impact and Fourier transform automatically satisfies trivial initial conditions. The forward and inverse Fourier transform are defined, respectively, as follows:

$$\tilde{u}(x,\omega) = \int_{-\infty}^{\infty} u(x,t) \cdot e^{-i\omega t} dt \qquad (100)$$

$$u(x,t) = \frac{1}{2\pi} \int_{-\infty}^{\infty} \tilde{u}(x,\omega) \cdot e^{i\omega t} d\omega \qquad (101)$$

By applying the Fourier transform over time, the governing equation becomes:

$$\tilde{u}_1'' + k^2 \tilde{u}_1 = 0 \qquad \text{for } x < x_A \qquad (102)$$

$$\tilde{u}_2'' + k^2 \tilde{u}_2 = 0 \qquad \text{for } x > x_A \qquad (103)$$

$$\tilde{u}_1 = \tilde{u}_2 \qquad \text{at } x = x_A \qquad (104)$$

$$\tilde{u}_1' - \tilde{u}_2' = \frac{1}{\rho A c^2} \qquad \text{at } x = x_A \qquad (105)$$

$$-c^2 \tilde{u}_1' + i\omega \varepsilon_{B,0} \tilde{u}_1 = 0 \qquad \text{at } x = 0 \qquad (106)$$

$$c^2 \tilde{u}_2' + i\omega \varepsilon_{B,L} \tilde{u}_2 = 0 \qquad \text{at } x = L \qquad (107)$$

- $k = \dfrac{\sqrt{\omega^2 - \omega_0^2}}{c}$ and the radical's branch points are defined as in eq. (44)

The general solutions to the equations of motion, eq. (102) and (103), are:

$$\tilde{u}_1(x,\omega) = C_1 \cdot e^{-ikx} + C_2 \cdot e^{ikx} \qquad \text{for } x < x_A \qquad (108)$$

$$\tilde{u}_2(x,\omega) = C_3 \cdot e^{-ikx} + C_4 \cdot e^{ikx} \qquad \text{for } x > x_A \qquad (109)$$

In this case, the general non-reflective boundaries, eq. (110), are going to be employed because of the propagating character of the solution. Consequently, $C_1 = C_4 = 0$.

$$\varepsilon_{B,0} = \varepsilon_{B,L} = \frac{kc^2}{\omega} \qquad (110)$$

Replacing the general solutions into the interface and boundary conditions, and by replacing the name of the functions from $u \to G$, the Green's functions are obtained.

$$\tilde{G}(x, x_A, \omega) = \frac{1}{2} \frac{1}{\rho A c^2} \frac{1}{ik} e^{-ik|x - x_A|} \qquad (111)$$

It must be mentioned that the only information needed is at the left boundary, $x = 0$, and because $x_A \geq 0$, the space derivative should be applied to the Green's function of the first domain. By doing so and evaluating it at $x = 0$, the Green's contribution in the eq. (108) is found.

$$\tilde{G}'(x = 0, x_A, \omega) = \frac{1}{2} \frac{1}{\rho A c^2} e^{-ikx_A} \qquad (112)$$

This function cannot be easily brought to the time domain analytically, because the wavenumber in the exponent contains the square root of frequency. Thus, the only way to apply the inverse is numerically.

4.3. Initial state

In order to find the initial state, the first derivative of Green's function has to be multiplied with the steady-state eigenfield evaluated at $x=0$. The Green's function and its derivative have been found in the previous subchapter, but the derived expressions are in the Fourier domain, while the expressions of the eigenfield are in the time domain. There are two possibilities, either apply the inverse Fourier transform to the first derivative of Green's function and perform the convolution in the time domain, or take the eigenfield to the Fourier domain, perform the multiplication and apply the inverse transform to obtain the result in the time domain. Although the first case requires less steps, taking the inverse Fourier transform of the first derivative of Green's function might introduce big errors. That is the reason why the second choice is preferred in this additional thesis.

In order to proceed and find the initial state, the expression of the eigenfield in the Fourier domain has to be found. The expression of the eigenfield in the time domain, evaluated at $x=0$ is presented below.

$$u\left(x=0,t\right)=\frac{1}{2}\frac{F_0}{\rho A}\frac{\beta}{\omega_0^{\,2}}\exp\left(-\beta v\left|t\right|\right) \tag{113}$$

Making use of the following property of Fourier transform,

$\exp\left(-a\left|t\right|\right)\xrightarrow{Fourier}\frac{2a}{a^2+\omega^2}$ provided that a is constant and $\mathrm{Re}\left(a\right)>0$, the expression of the eigenfield in the Fourier domain is found.

$$\tilde{u}_{in}\left(x=0,\omega\right)=\frac{1}{2}\frac{F_0}{\rho A}\frac{\beta}{\omega_0^{\,2}}\frac{2\beta v}{\beta^2v^2+\omega^2} \tag{114}$$

Now, all the components needed to find the initial state using the reciprocity relation, are derived. Substituting the expression of the first derivative of Green's function evaluated at $x=0$, eq. (112), and the expression of the inward propagating displacement field also evaluated at $x=0$, eq. (114), into eq. (93), the displacement field expression derived by means of reciprocity theorem is found.

$$\tilde{u}\left(x_A,\omega\right)=\frac{1}{2}\frac{F_0}{\rho A}\frac{\beta}{\omega_0^{2}}\frac{2\beta v}{\beta^2v^2+\omega^2}\mathrm{e}^{-ikx_A} \tag{115}$$

Now this expression needs to be brought to the time domain by applying the inverse Fourier transform numerically. For the solution to converge, a small amount of damping has to be added to the system. The slightly changed equations are described in Annex 2.

In the case of varying external stiffness, the information about the change in stiffness is contained in the Green's function.

4.4. Graphical results

First, as a validation of the numerical model, the initial displacement derived by means of reciprocity relation is plotted against the steady-state eigenfield in the case of constant external stiffness.

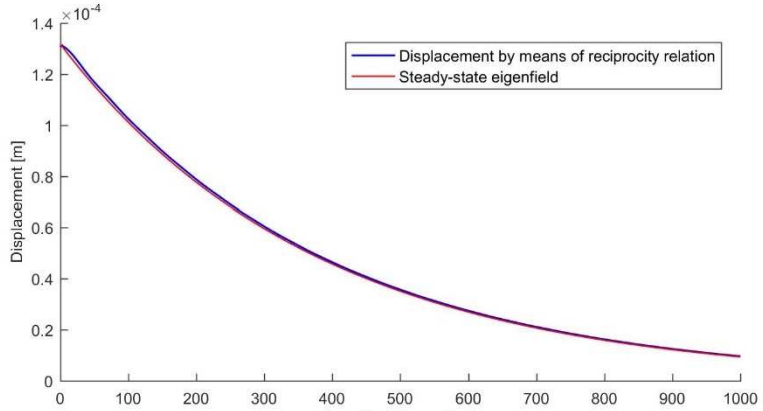

Figure 20 – Initial displacement derived by means of reciprocity relation plotted against the steady-state eigenfield for constant external stiffness

As it can be seen from the above figure, the displacement field derived by means of the reciprocity relation is almost the same as the exact, steady-state, eigenfield. The most noticeable difference is at the tip, where in order to obtain such a sharp angle as the eigenfield, the frequency truncation in the inverse Laplace has to be very large.

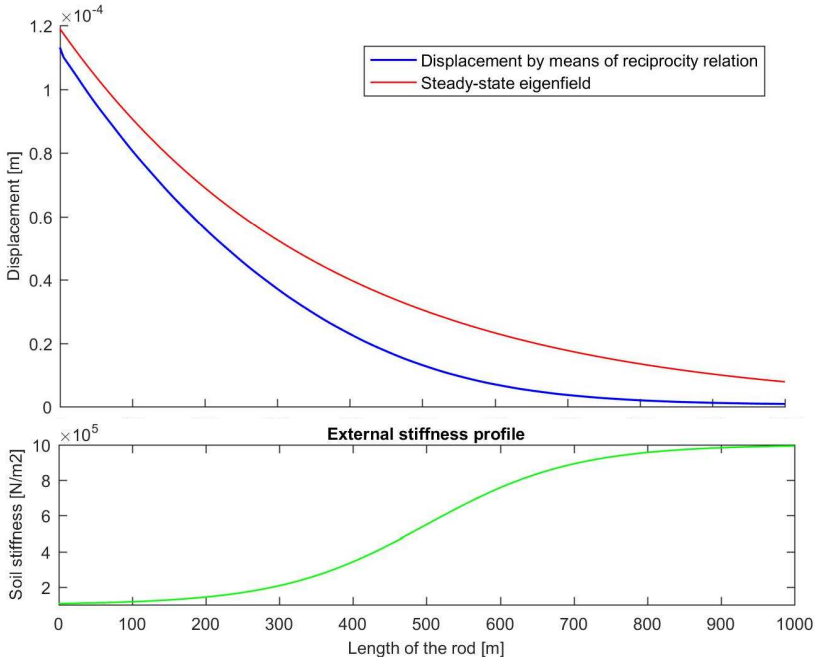

Figure 21 - Initial displacement derived by means of reciprocity relation plotted against the steady-state eigenfield for varying external stiffness

The initial displacement field for the case of varying stiffness is presented in Figure 21. The steady-state eigenfield is plotted as well as a reference point, with the constant stiffness equal to the stiffness at $x = 0$ from the varying stiffness system. It should be noted that although at $x = 0$ both systems have the same external stiffness, the displacements are not the same. This comes as no surprise because the high external stiffness present in the second half of the domain acts almost like a clamping, thus affecting displacements of the rod at $x = 0$ as well, through the internal stiffness of the rod.

5. Graphical results

The plots in the following figures represent snapshots of the computational domain for several time moments. The values of the coefficients used in the plots are the following:

$$\rho = 8050\left[kg/m^3\right] \qquad k_1 = 1\cdot 10^5\left[N/m^2\right]$$
$$E = 2.1\cdot 10^{11}\left[N/m^2\right] \qquad k_2 = 1\cdot 10^6\left[N/m^2\right]$$
$$A = 0.09\left[m^2\right] \qquad F_0 = 1\cdot 10^4\left[N\right]$$

The system is plotted for two velocities of the load, $v = 0.7\cdot c$ and $v = 0.95\cdot c$, to observe this influence on the displacements. Also, the system is plotted for a more abrupt stiffness change in the case of load velocity $v = 0.95\cdot c$.

We can observe, in Figure 24, that the eigenfield does becomes smaller as it transitions to the stiff part of the domain. But the waves propagating away from the disturbance are not so obvious in the case of the load velocity $v = 0.7\cdot c$. These waves can be observed in the middle right plot and the bottom two, in the bottom right one being quite clear. The displacements in the left half of the domain have become negative which is a sign of these waves.

In the case of velocity $v = 0.95\cdot c$, Figure 23, the waves propagated from the transition are clearer. This is because, as the load approaches the wave speed in the rod, there is an amplification of the displacements, a type of resonance. It must be noted that also the eigenfield displacement gets larger for higher load velocity. But, the waves become clearer because they also amplify relative to the eigenfield.

In Figure 24, the same load velocity is used, $v = 0.95\cdot c$, but the stiffness transition is more abrupt. This situation also amplifies the magnitude of the displacements. Although it was not presented in this additional thesis, one should realize that the eigenfield possess a certain amount of energy. As we have seen, the eigenfield is the steady- steady solution of the system with constant external stiffness. Consequently, the system will have two eigenfields, before and after the stiffness transition. The difference in energy possessed by the two eigenfields represents exactly the energy radiated at the transition. Thus, if the abruptness of the transition increases, the same amount of energy is going to be radiated in a shorter amount of time, leading to larger displacements and stresses in the rod. This can be seen between Figure 23 and Figure 24.

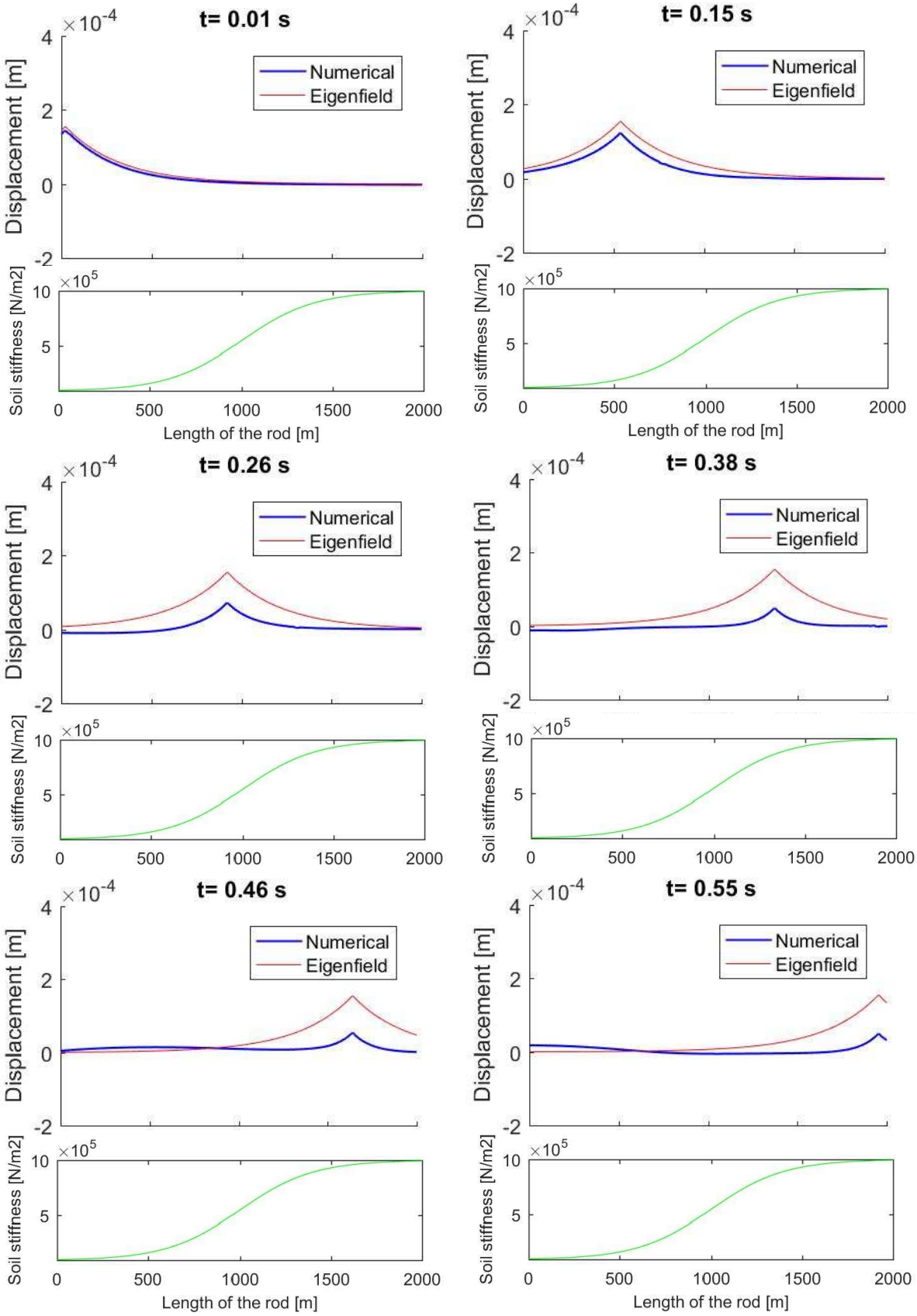

Figure 22 - Numerical results of the model with varying stiffness for v = 0.7 c

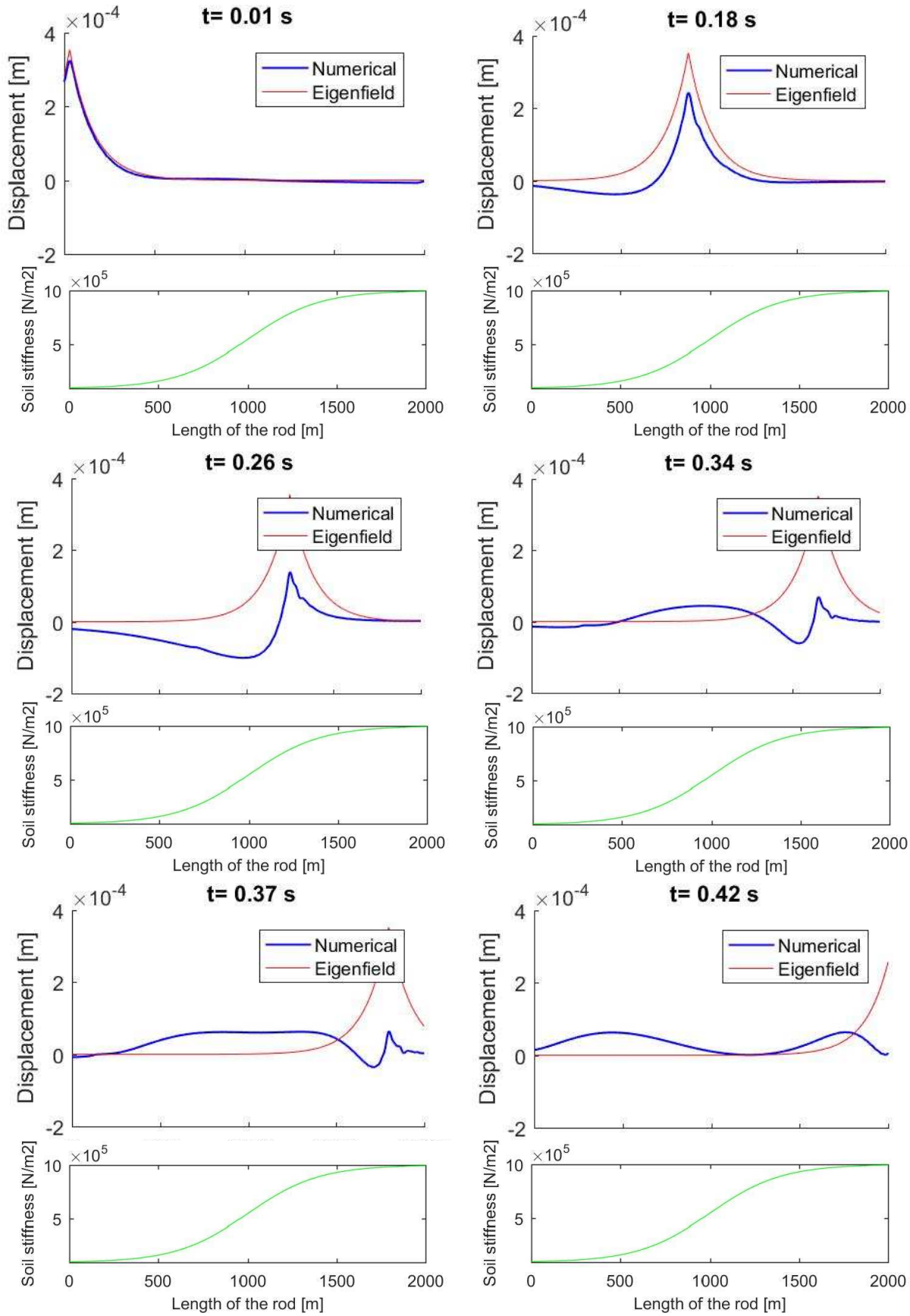

Figure 23 - Numerical results of the model with varying stiffness for v = 0.95 c

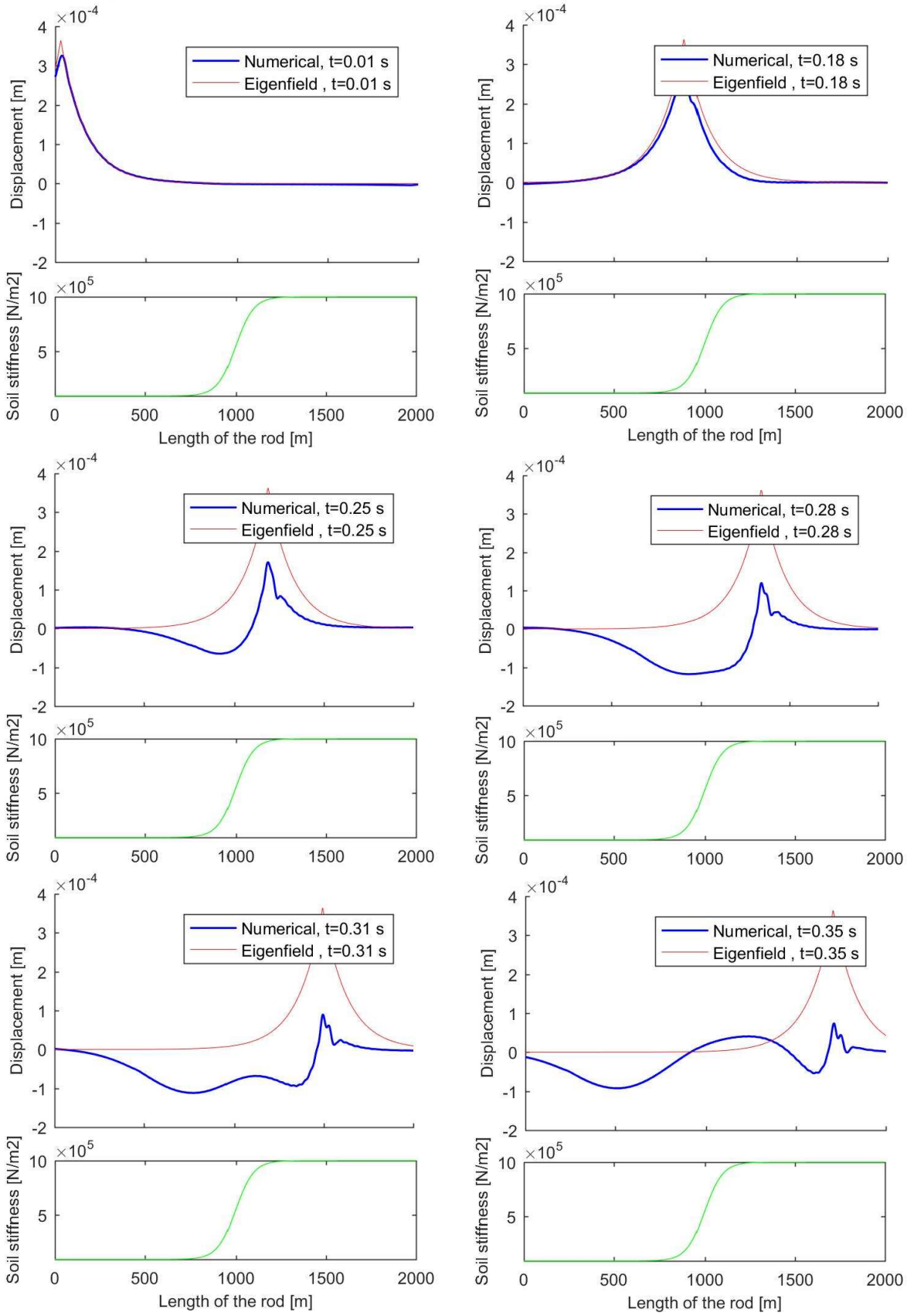

Figure 24 - Numerical results of the model with varying stiffness for v = 0.95 c

6. Conclusions

The goal of this additional thesis was to construct a one-dimensional model of a finite rod resting on elastic foundation with smooth varying stiffness, subjected to a uniformly moving constant load in order to observe the transition radiation phenomenon. To achieve this goal, several challenges have been overcome.

First, in order to reduce the computational domain as much as possible, the initial state of the already disturbed domain had to be found. For this we made use of the Reciprocity theorem. The general reciprocity relation for the rod was derived. Assuming non-reflective boundaries and splitting the Green's function into inward and outward propagating fields it was simplified. Afterwards, the Green's function was derived in the Fourier domain. In order to minimize the numerical error, the steady-state eigenfield was taken to the Fourier domain, performed the multiplication and applied the inverse Fourier transform numerically to the whole relation. Although the results were good, when compared against the analytical solution (in the case of constant stiffness), because of frequency truncation, the tip of the displacement doesn't exhibit such a sharp angle.

Secondly, in order to truly represent an infinite system, we derived non-reflective boundaries for each of the analysis performed. For both the transient cases, with trivial initial conditions and 'tuned' initial conditions, the non-reflective boundary coefficients found were the expected ones, but in order to obtain them we had to change the system into a semi-infinite one because the removal of the load was introducing additional transient waves. Lastly, the non-reflective boundary for both the eigenfield and the transients turned out to be unexpected. Although the combination of the two elements composing the boundary, spring and dashpot, results in the general non-reflective boundary, the initial state present in the boundary condition has to be accounted only for the dashpot.

Finally, the two parts were put together to construct the model, which provided expected insights about the phenomenon, thus validating the model. We can see in the plots from chapter 5 that as the load velocity approaches the wave velocity in the rod, the displacements get amplified with respect to the eigenfield. Also, as the transition in stiffness gets more abrupt, the displacements are observed to increase. These results were already known, but the goal of this additional thesis was to develop the model, not so much to analyze new behaviour.

7. Bibliography

Wolfert A.R.M., 1999. *Wave effects in one-dimensional elastic systems interacting with moving loads.* Thesis TU-Delft, DUP Science, Delft

Achenbach J.D., 2003. *Reciprocity in elastodynamics*. Cambridge University Press, 2003

A.V. Metrikine, A.C.W.M. Vrouwenvelder. *Dynamics of Structures* – CT4140 Lecture Notes. Delft University of Technology

K.N. van Dalen, 2006. *Transition radiation in two-dimensional inhomogeneous elastic systems.* Thesis TU-Delft

Kampas G., 2007. *Basic transfer and time-response functions of the three parameter fluid and solid viscoelastic model.* Dissertation, University of Patras, Greece

Kees Wapenaar, Joost van der Neut, Elmer Ruigrok, Deyan Draganov, Jurg Hunziker, Evert Slob, Jan Thorbecke, Roel Snieder, 2010. Seismic interferometry by crosscorrelation and by multi-dimensional deconvolution: a systematic comparison. Geophys. J. Int. (2010) 183, pag. 3

Annex 1. Transient solution for the case with additional distributed damping

If there is external damping added to the system, the equations of motion in the time domain change to:

$$\ddot{u}_1 - c^2 u_1'' + \varepsilon_d \dot{u}_1 + \omega_0^2 u_1 = 0 \qquad \text{for } x = (-l, 0) \tag{116}$$

$$\ddot{u}_2 - c^2 u_2'' + \varepsilon_d \dot{u}_2 + \omega_0^2 u_2 = 0 \qquad \text{for } x = (0, \infty) \tag{117}$$

- ε_d represents the distributed external viscous damping divided by ρA

The interface and boundary conditions remain unchanged because a distributed system property does not show up in the localized conditions.

The equations of motion in Laplace domain read:

$$\tilde{u}_1'' + R^2 \tilde{u}_1 = -\frac{1}{c^2}\left(s u_1(t=0) + \varepsilon_d u_1(t=0) + \dot{u}_1(t=0)\right) \tag{118}$$

$$\tilde{u}_2'' + R^2 \tilde{u}_2 = -\frac{1}{c^2}\left(s u_2(t=0) + \underbrace{\varepsilon_d u_2(t=0)}_{\text{contribution from the distributed damping}} + \dot{u}_2(t=0) + \frac{F_0}{\rho A}\frac{1}{v} e^{-\frac{s}{v}x} \right) \tag{119}$$

- $R = \dfrac{\sqrt{-s^2 - s\varepsilon_d - \omega_0^2}}{c} \xrightarrow{s=i\omega} \dfrac{\sqrt{\omega^2 - i\omega\varepsilon_d - \omega_0^2}}{c}$ the wavenumber

The branches of the complex radicals are chosen in such a way that they fulfill the following requirement:

$$\operatorname{Im}\left\{\sqrt{\omega^2 - i\omega\varepsilon_d - \omega_0^2}\right\} < 0, \qquad \forall \omega \in \mathbb{R} \tag{120}$$

In the case of trivial initial conditions, the general solutions, after accounting for the proper behaviour for $x \to \infty$, are:

$$\tilde{u}_1(x,s) = C_1 \cdot e^{-iRx} + C_2 \cdot e^{iRx} \tag{121}$$

$$\tilde{u}_2(x,s) = C_3 \cdot e^{-iRx} - \frac{F_0}{\rho A c^2}\frac{1}{v}\frac{1}{\frac{s^2}{v^2} + R^2} e^{-\frac{s}{v}x} \tag{122}$$

Substituting these solutions, eq. (121) and (122), into the interface conditions and boundary condition, eq. (35) - (37), the three unknowns can be found from this system of algebraic equations. Applying the condition that $C_1 = 0$, the same form of the non-reflective boundary is found as in the case without damping, except that the wavenumber expression contains the damping term as well:

$$\varepsilon_{b,-l} = \frac{iRc^2}{s} \tag{123}$$

The solutions now become:

$$\tilde{u}_1(x,s) = \frac{1}{2}\frac{F_0}{\rho A c^2}\frac{1}{iR(s+iRv)}e^{iRx} \tag{124}$$

$$\tilde{u}_2(x,s) = \frac{1}{2}\frac{F_0}{\rho A c^2}\frac{1}{iR(s-iRv)}e^{-iRx} - \frac{F_0}{\rho A c^2}\frac{1}{v}\frac{1}{\frac{s^2}{v^2}+R^2}e^{-\frac{s}{v}x} \tag{125}$$

In the case where the initial conditions are chosen such that no transients are excited due to the load entry, first the steady-state eigenfield changed expressions are going to be derived. The kinematic invariant, eq. (11), remains unchanged, while the dispersion equation, eq. (9), changes to:

$$c^2 \cdot k^2 - \omega^2 + \omega_0^2 + i\varepsilon_d\omega = 0 \tag{126}$$

Solving this system of two equations the frequency and wavenumber are found, for the subsonic case, to be:

$$\omega_{1,2} = i\beta_{1,2}v \tag{127}$$

$$k_{1,2} = i\beta_{1,2} \tag{128}$$

- $$\beta_1 = \frac{-\frac{\varepsilon_d}{2}v + \omega_0\sqrt{c^2 - v^2\cdot\left(1-\left(\frac{\varepsilon_d}{2\omega_0}\right)^2\right)}}{c^2 - v^2} \tag{129}$$

- $$\beta_2 = \frac{-\frac{\varepsilon_d}{2}v - \omega_0\sqrt{c^2 - v^2\cdot\left(1-\left(\frac{\varepsilon_d}{2\omega_0}\right)^2\right)}}{c^2 - v^2} \tag{130}$$

It can be seen from the above expressions that for the case of added damping the subsonic and supersonic cases are defined depending on the magnitude of the wave speed, c, with respect to $v\cdot\sqrt{1-\left(\frac{\varepsilon_d}{2\omega_0}\right)^2}$.

Following the same steps as explained in chapter 3.1 the expression for the eigenfield is found.

$$u_1(x,t) = \frac{1}{2}\frac{F_0}{\rho A}\frac{1}{r}e^{\beta_1(x-vt)}, \qquad u_2(x,t) = \frac{1}{2}\frac{F_0}{\rho A}\frac{1}{r}e^{\beta_2(x-vt)} \tag{131}$$

- where $r = \omega_0 \sqrt{c^2 - v^2 \cdot \left(1 - \left(\frac{\varepsilon_d}{2\omega_0}\right)^2\right)}$

Now, the initial conditions to be employed in the solutions are:

$$u_1(x, t=0) = \frac{1}{2}\frac{F_0}{\rho A}\frac{1}{r}e^{\beta_1 x} \quad , \quad \dot{u}_1(x, t=0) = -\frac{1}{2}\frac{F_0}{\rho A}\frac{\beta_1 v}{r}e^{\beta_1 x} \tag{132}$$

$$u_2(x, t=0) = \frac{1}{2}\frac{F_0}{\rho A}\frac{1}{r}e^{\beta_2 x} \quad , \quad \dot{u}_2(x, t=0) = -\frac{1}{2}\frac{F_0}{\rho A}\frac{\beta_2 v}{r}e^{\beta_2 x} \tag{133}$$

The equations of motion, eq. (118) and (119), become:

$$\tilde{u}_1'' + R^2\tilde{u}_1 = -\frac{1}{2}\frac{F_0}{\rho A c^2}\frac{s + \varepsilon_d - \beta_1 v}{r}e^{\beta_1 x} \tag{134}$$

$$\tilde{u}_2'' + R^2\tilde{u}_2 = -\frac{1}{2}\frac{F_0}{\rho A c^2}\frac{s + \varepsilon_d - \beta_2 v}{r}e^{\beta_2 x} - \frac{F_0}{\rho A c^2}\frac{1}{v}e^{-\frac{s}{v}x} \tag{135}$$

The general solutions to these equations of motion are:

$$\tilde{u}_1(x, s) = C_1 \cdot e^{-iRx} + C_2 \cdot e^{iRx} - \frac{1}{2}\frac{F_0}{\rho A c^2}\frac{1}{r}\frac{s + \varepsilon_d - \beta_1 v}{\beta_1^2 + R^2}e^{\beta_1 x} \tag{136}$$

$$\tilde{u}_2(x, s) = C_3 \cdot e^{-iRx} - \frac{1}{2}\frac{F_0}{\rho A c^2}\frac{1}{r}\frac{s + \varepsilon_d - \beta_2 v}{\beta_2^2 + R^2}e^{\beta_2 x} - \frac{F_0}{\rho A c^2}\frac{1}{v}\frac{1}{\frac{s^2}{v^2} + R^2}e^{-\frac{s}{v}x} \tag{137}$$

Once again, substituting these solutions into the interface conditions and boundary condition, eq. (35) - (37), the three unknowns can be found from this system of algebraic equations. Applying the condition that $C_1 = 0$, the non-reflective boundary is found which has a more complicated expression this time, but by employing it, all constants turn to zero. Consequently, the final expression in the Laplace domain are:

$$\tilde{u}_1(x, s) = -\frac{1}{2}\frac{F_0}{\rho A c^2}\frac{1}{r}\frac{s + \varepsilon_d - \beta_1 v}{\beta_1^2 + R^2}e^{\beta_1 x} \tag{138}$$

$$\tilde{u}_2(x, s) = -\frac{1}{2}\frac{F_0}{\rho A c^2}\frac{1}{r}\frac{s + \varepsilon_d - \beta_2 v}{\beta_2^2 + R^2}e^{\beta_2 x} - \frac{F_0}{\rho A c^2}\frac{1}{v}\frac{1}{\frac{s^2}{v^2} + R^2}e^{-\frac{s}{v}x} \tag{139}$$

These expressions are brought to the time domain using trapezoidal rule to approximate the integrals (52) and (53).

Annex 2. Initial state derived by means of reciprocity method for the case with additional distributed damping

The time domain expressions of the eigenfield in the case with distributed damping have been derived in Annex 1. It must be noted that because this analysis is carried out for $t \le 0$, thus the load is always outside the domain, the only relevant part of the eigenfield is the one in front of the load. Consequently, evaluating the eigenfield for domain two (eq. 131) at $x = 0$ results in the following expression:

$$u_{in}(x=0,t) = \frac{1}{2}\frac{F_0}{\rho A}\frac{1}{r}e^{\beta_2 v|t|} \tag{140}$$

- where $\beta_2 = \dfrac{-\frac{\varepsilon_d}{2}v - \omega_0\sqrt{c^2 - v^2\cdot\left(1-\left(\frac{\varepsilon_d}{2\omega_0}\right)^2\right)}}{c^2 - v^2}$
- and $r = \omega_0\sqrt{c^2 - v^2\cdot\left(1-\left(\frac{\varepsilon_d}{2\omega_0}\right)^2\right)}$

To find the Fourier transform of eq. (140), the same reasoning is applied as in the case without damping. Making use of the following property of Fourier transform,

$\exp(-a|t|) \xrightarrow{Fourier} \dfrac{2a}{a^2+\omega^2}$ provided that a is constant and $\mathrm{Re}(a) > 0$, the expression of the eigenfield in the Fourier domain is found.

$$\tilde{u}_{in}(x=0,\omega) = \frac{1}{2}\frac{F_0}{\rho A}\frac{1}{r}\frac{-2\beta_2 v}{\beta_2^2 v^2 + \omega^2} \tag{141}$$

The expressions of the Green's function and the first derivative are the same, just the wavenumber changes to include the damping as well:

$$k = \frac{\sqrt{\omega^2 - i\omega\varepsilon_d - \omega_0^2}}{c} \tag{142}$$

Substituting eq. (141) and eq. (112) with the wavenumber definition from eq. (142), into eq. (93), the displacement field in Fourier domain is found.

$$\tilde{u}(x_A,\omega) = \frac{1}{2}\frac{F_0}{\rho A}\frac{1}{r}\frac{-2\beta v}{\beta^2 v^2 + \omega^2}\exp(-ikx_A) \tag{143}$$

After taking the numerical inverse Fourier transform of the expression (143) the displacement field in the time domain is found. The results are presented in chapter 4.4.

Annex 3. Finite difference numerical model

The procedure how the Finite difference method was used in developing the varying stiffness model is going to be exemplified on a rod divided in 6 elements as in the figure below.

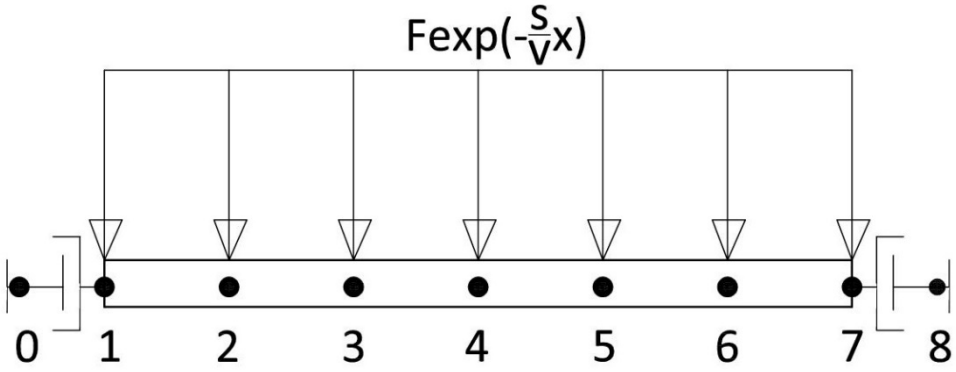

Figure 25 – Finite Difference Method for approximating the second order derivative with respect to x

Note that we are approximating the second derivative with respect to space to the equation of motion in Laplace domain. Consequently, the force is acting on the whole domain.

The first and second derivative approximations using Finite difference method are:

$$u_n'' = \frac{1}{l^2}\left(u_{n-1} - 2u_n + u_{n+1}\right) \tag{144}$$

$$u_n' = \frac{1}{2l}\left(u_{n+1} - u_{n-1}\right) \quad \text{(central difference)} \tag{145}$$

- $l = \frac{L}{N}$ represents the length of one element, L the length of the rod, N the number of elements

The only remaining challenge now is to find the expressions for the boundary elements, for which the ghost nodes are going to be used. The boundary conditions are:

$$-c^2\tilde{u}_1' + s\varepsilon_b\tilde{u}_1 = \frac{F}{2} \tag{146}$$

$$c^2\tilde{u}_7' + s\varepsilon_b\tilde{u}_7 = \frac{F}{2} \tag{147}$$

Substituting the expression for the first derivative, eq. (145), into the boundary conditions and expressing the ghost nodes explicitly we find:

$$u_0 = u_2 - \frac{2\varepsilon_b l}{c^2}u_1 + \frac{Fl}{c^2} \tag{148}$$

$$u_8 = u_6 - \frac{2\varepsilon_b l}{c^2}u_7 + \frac{Fl}{c^2} \tag{149}$$

Now the second derivative of the first and last nodes become:

$$u_1'' = \frac{1}{l^2}\left(-2\left(1+\frac{\varepsilon_b l}{c^2}\right)u_1 + 2u_2\right) + \frac{F}{l} \tag{150}$$

$$u_7'' = \frac{1}{l^2}\left(-2\left(1+\frac{\varepsilon_b l}{c^2}\right)u_7 + 2u_6\right) + \frac{F}{l} \tag{151}$$

The whole matrix of second derivatives becomes:

$$K = \frac{1}{l^2}\begin{pmatrix} -2\left(1+\frac{\varepsilon_b l}{c^2}\right) & 2 & 0 & 0 & 0 & 0 & 0 \\ 1 & -2 & 1 & 0 & 0 & 0 & 0 \\ 0 & 1 & -2 & 1 & 0 & 0 & 0 \\ 0 & 0 & 1 & -2 & 1 & 0 & 0 \\ 0 & 0 & 0 & 1 & -2 & 1 & 0 \\ 0 & 0 & 0 & 0 & 1 & -2 & 1 \\ 0 & 0 & 0 & 0 & 0 & 2 & -2\left(1+\frac{\varepsilon_b l}{c^2}\right) \end{pmatrix} \tag{152}$$

And the whole system of equations that needs to be solved with respect to displacements:

$$\left[\frac{-c^2}{l^2}\begin{pmatrix} -2\left(1+\frac{\varepsilon_b l}{c^2}\right) & 2 & 0 & 0 & 0 & 0 & 0 \\ 1 & -2 & 1 & 0 & 0 & 0 & 0 \\ 0 & 1 & -2 & 1 & 0 & 0 & 0 \\ 0 & 0 & 1 & -2 & 1 & 0 & 0 \\ 0 & 0 & 0 & 1 & -2 & 1 & 0 \\ 0 & 0 & 0 & 0 & 1 & -2 & 1 \\ 0 & 0 & 0 & 0 & 0 & 2 & -2\left(1+\frac{\varepsilon_b l}{c^2}\right) \end{pmatrix} + \frac{1}{\rho A}\begin{pmatrix} k^2(x_1) & 0 & 0 & 0 & 0 & 0 & 0 \\ 0 & k^2(x_2) & 0 & 0 & 0 & 0 & 0 \\ 0 & 0 & k^2(x_3) & 0 & 0 & 0 & 0 \\ 0 & 0 & 0 & k^2(x_4) & 0 & 0 & 0 \\ 0 & 0 & 0 & 0 & k^2(x_5) & 0 & 0 \\ 0 & 0 & 0 & 0 & 0 & k^2(x_6) & 0 \\ 0 & 0 & 0 & 0 & 0 & 0 & k^2(x_7) \end{pmatrix}\right]\begin{pmatrix} u_1 \\ u_2 \\ u_3 \\ u_4 \\ u_5 \\ u_6 \\ u_7 \end{pmatrix} = \begin{pmatrix} -\frac{F_1}{l} \\ F_2 \\ F_3 \\ F_4 \\ F_5 \\ F_6 \\ -\frac{F_7}{l} \end{pmatrix}$$

Where the forcing in the specific forcing at that node.

$$F_1 = \frac{F_0}{\rho A}\frac{1}{v}e^{-\frac{s}{v}x_1}$$